2. Bancroft JD, Stevens A. Theory and practice of histological techniques, Vol. 1. London: Churchill Livingstone; 1996. p 343–364.
3. Banwell BL, Russel J, Fukudome T, Shen XM, Stilling G, Engel AG. Myopathy, myasthenic syndrome, and epidermolysis bullosa simplex due to plectin deficiency. J Neuropathol Exp Neurol 1999;58:832–846.
4. Carlsson L, Li ZL, Paulin D, Price MG, Breckler J, Robson RM, et al. Differences in the distribution of synemin, paranemin, and plectin in skeletal muscles of wild-type and desmin knockout mice. Histochem Cell Biol 2000;114:39–47.
5. Charlesworth A, Gagnoux-Palacios L, Bonduelle M, Ortonne J-P, De Raeve L, Meneguzzi G. Identification of a lethal form of epidermolysis bullosa simplex associated with a homozygous genetic mutation in plectin. J Invest Dermatol 2004;121: 1344–1348.
6. Costa ML, Escaleira R, Cataldo A, Oliveira F, Mermelstein CS. Desmin: molecular interactions and putative functions of the muscle intermediate filament protein. Braz J Med Biol Res 2004;37:1819–1830.
7. Elliott CE, Becker B, Oehler S, Castanon MJ, Hauptmann R, Wiche G. Plectin transcript diversity: identification and tissue distribution of variants with distinct first coding exons and rodless isoforms. Genomics 1997;42:115–125.
8. Foisner R, Feldman B, Sander L, Seifert G, Artlieb U, Wiche G. A panel of monoclonal antibodies to rat plectin: distinction by epitope mapping and immunoreactivity with different tissues and cell lines. Acta Histochem 1994;96:421–438.
9. Foisner R, Feldman B, Sander L, Wiche G. Monoclonal antibody mapping of structural and functional plectin epitopes. J Cell Biol 1991;112:397–405.
10. Fuchs P, Zorer M, Rezniczek GA, Spazierer D, Oehler S, Castanon MJ, et al. Unusual 5' transcript complexity of plectin isoforms: novel tissue-specific exons modulate actin binding activity. Hum Mol Genet 1999;8:2461–2472.
11. Gache Y, Chavanas S, Lacour JP, Wiche G, Owaribe K, Meneguzzi G, et al. Defective expression of plectin/hd1 in epidermolysis bullosa simplex with muscular dystrophy. J Clin Invest 1996;97:2289–2298.
12. Gauthier GF. Ultrastructural identification of muscle fiber types by immunocytochemistry. J Cell Biol 1979;82:391–400.
13. Gauthier GF, Lowey S. Distribution of myosin isoenzymes among skeletal muscle fiber types. J Cell Biol 1979;81:10–25.
14. Goebel HH. Desmin-related neuromuscular disorders. Muscle Nerve 1995;18:1306–1320.
15. Hieda Y, Nishizawa Y, Uematsu J, Owaribe K. Identification of a new hemidesmosomal protein, hd1: a major, high molecular mass component of isolated hemidesmosomes. J Cell Biol 1992;116:1497–1506.
16. Hijikata T, Murakami T, Imamura M, Fujimaki N, Ishikawa H. Plectin is a linker of intermediate filaments to z-discs in skeletal muscle fibers. J Cell Sci 1999;112:867–876.
17. Hijikata T, Murakami T, Ishikawa H, Yorifuji H. Plectin tethers desmin intermediate filaments onto subsarcolemmal dense plaques containing dystrophin and vinculin. Histochem Cell Biol 2003;119:109–123.
18. Karnovsky MJA. Formaldehyde-glutaraldehyde fixative of high osmolarity for use in electron microscopy. J Cell Biol 1965;27:137–138a.
19. Koss-Harnes D, Hoyheim B, Anton-Lamprecht I, Gjesti A, Jorgensen RS, Jahnsen FL, et al. A site-specific plectin mutation causes dominant epidermolysis bullosa simplex ogna: two identical de novo mutations. J Invest Dermatol 2002;118:87–93.
20. Koss-Harnes D, Jahnsen FL, Wiche G, Soyland E, Brandtzaeg P, Gedde-Dahl T, Jr. Plectin abnormality in epidermolysis bullosa simplex ogna: non-responsiveness of basal keratinocytes to some anti-rat plectin antibodies. Exp Dermatol 1997; 6:41–48.
21. Koster J, Geerts D, Favre B, Borradori L, Sonnenberg A. Analysis of the interactions between BP180, BP230, plectin and the integrin alpha6beta4 important for hemidesmosome assembly. J Cell Sci 2003;116:387–399.
22. Koster J, van Wilpe S, Kuikman I, Litjens SH, Sonnenberg A. Role of binding of plectin to the integrin beta4 subunit in the assembly of hemidesmosomes. Mol Biol Cell 2004;15:1211–1223.
23. Litjens SH, Wilhelmsen K, de Pereda JM, Perrakis A, Sonnenberg A. Modeling and experimental validation of the binary complex of the plectin actin binding domain and the first pair of fnIII domains of the $\beta 4$ integrin. J Biol Chem 2005;280: 22270–22277.
24. Liu CG, Maercker C, Castanon MJ, Hauptmann R, Wiche G. Human plectin: organization of the gene, sequence analysis, and chromosome localization (8q24). Proc Natl Acad Sci U S A 1996;93:4278–4283.
25. McLean WHI, Pulkkinen L, Smith FJ, Rugg EL, Lane EB, Bullrich F, et al. Loss of plectin causes epidermolysis bullosa with muscular dystrophy: cDNA cloning and genomic organization. Genes Dev 1996;10:1724–1735.
26. McMillan JR, Akiyama M, Nakamura H, Shimizu H. Colocalization of multiple laminin isoforms predominantly beneath hemidesmosomes in the upper lamina densa of the epidermal basement membrane. J Histochem Cytochem 2006;54:109–111.
27. McMillan JR, Eady RA. Hemidesmosome ontogeny in digit skin of the human fetus. Arch Dermatol Res 1996;288:91–97.
28. McMillan JR, McGrath JA, Tidman MJ, Eady RA. Hemidesmosomes show abnormal association with the keratin filament network in junctional forms of epidermolysis bullosa. J Invest Dermatol 1998;110:132–137.
29. Mellerio JE, Smith FJ, McMillan JR, McLean WHI, McGrath JA, Morrison GA, et al. Recessive epidermolysis bullosa simplex associated with plectin mutations: infantile respiratory complications in two unrelated cases. Br J Dermatol 1997;137: 898–906.
30. Nakamura H, Sawamura D, Goto M, McMillan JR, Park S, Kono S, et al. Epidermolysis bullosa simplex associated with pyloric atresia is a novel clinical subtype caused by mutations in the plectin gene (plec1). J Mol Diagn 2005;7:28–35.
31. Okumura M, Uematsu J, Hirako Y, Nishizawa Y, Shimizu H, Kido N, et al. Identification of the hemidesmosomal 500 kda protein (hd1) as plectin. J Biochem (Tokyo) 1999;126:1144–1150.
32. Osmanagic-Myers S, Wiche G. Plectin-rack1 (receptor for activated c kinase 1) scaffolding: a novel mechanism to regulate protein kinase c activity. J Biol Chem 2004;279:18701–18710.
33. Pfendner E, Uitto J. Plectin gene mutations can cause epidermolysis bullosa with pyloric atresia. J Invest Dermatol 2005; 124:111–115.
34. Pulkkinen L, Smith FJ, Shimizu H, Murata S, Yaoita H, Hachisuka H, et al. Homozygous deletion mutations in the plectin gene (plec1) in patients with epidermolysis bullosa simplex associated with late-onset muscular dystrophy. Hum Mol Genet 1996;5:1539–1546.
35. Reimann J, Kunz WS, Vielhaber S, Kappes-Horn K, Schroder R. Mitochondrial dysfunction in myofibrillar myopathy. Neuropathol Appl Neurobiol 2003;29:45–51.
36. Rezniczek GA, Abrahamsberg C, Fuchs P, Spazierer D, Wiche G. Plectin 5'-transcript diversity: short alternative sequences determine stability of gene products, initiation of translation and subcellular localization of isoforms. Hum Mol Genet 2003;12:3181–3194.
37. Richardson KC, Jarret L, Finke EH. Embedding in epoxy resins for ultrathin sectioning in electron microscopy. Stain Technol 1960;35:313–323.
38. Schroder R, Kunz WS, Rouan F, Pfendner E, Tolksdorf K, Kappes-Horn K, et al. Disorganization of the desmin cytoskeleton and mitochondrial dysfunction in plectin-related epidermolysis bullosa simplex with muscular dystrophy. J Neuropathol Exp Neurol 2002;61:520–530.

39. Schroder R, Mundegar RR, Treusch M, Schlegel U, Blumcke I, Owaribe K, et al. Altered distribution of plectin/hd1 in dystrophinopathies. Eur J Cell Biol 1997;74:165–171.
40. Schroder R, Pacholsky D, Reimann J, Matten J, Wiche G, Furst DO, et al. Primary longitudinal adhesion structures: plectin-containing precursors of costameres in differentiating human skeletal muscle cells. Histochem Cell Biol 2002;118:301–310.
41. Schroder R, Warlo I, Herrmann H, van der Ven PF, Klasen C, Blumcke I, et al. Immunogold EM reveals a close association of plectin and the desmin cytoskeleton in human skeletal muscle. Eur J Cell Biol 1999;78:288–295.
42. Sevcik J, Urbanikova L, Kost'an J, Janda L, Wiche G. Actin-binding domain of mouse plectin. Crystal structure and binding to vimentin. Eur J Biochem 2004;271:1873–1884.
43. Shimizu H, Takizawa Y, Pulkkinen L, Murata S, Kawai M, Hachisuka H, et al. Epidermolysis bullosa simplex associated with muscular dystrophy: phenotype-genotype correlations and review of the literature. J Am Acad Dermatol 1999;41: 950–956.
44. Skalli O, Jones JC, Gagescu R, Goldman RD. Ifap 300 is common to desmosomes and hemidesmosomes and is a possible linker of intermediate filaments to these junctions. J Cell Biol 1994;125:159–170.
45. Smith FD, Eady RAJ, Leigh IM, McMillan JR, Rugg EL, Kelsell DP, et al. Plectin deficiency: hereditary basis for muscular dystrophy with epidermolysis bullosa. Nat Genet 1996;13:450–457.
46. Stegh AH, Herrmann H, Lampel S, Weisenberger D, Andra K, Seper M, et al. Identification of the cytolinker plectin as a major early in vivo substrate for caspase 8 during cd95- and tumor necrosis factor receptor-mediated apoptosis. Mol Cell Biol 2000;20:5665–5679.
47. Takizawa Y, Shimizu H, Rouan F, Kawai M, Udono M, Pulkkinen L, et al. Four novel plectin gene mutations in Japanese patients with epidermolysis bullosa with muscular dystrophy disclosed by heteroduplex scanning and protein truncation tests. J Invest Dermatol 1999;112:109–112.
48. Tanaka H, Hijikata T, Murakami T, Fujimaki N, Ishikawa H. Localization of plectin and other related proteins along the sarcolemma in smooth muscle cells of rat colon. Cell Struct Funct 2001;26:61–70.
49. Vita G, Monici MC, Owaribe K, Messina C. Expression of plectin in muscle fibers with cytoarchitectural abnormalities. Neuromuscul Disord 2003;13:485–492.
50. Wiche G. Role of plectin in cytoskeleton organization and dynamics. J Cell Sci 1998;111:2477–2486.
51. Wiche G, Krepler R, Artlieb U, Pytela R, Aberer W. Identification of plectin in different human cell types and immunolocalization at epithelial basal cell surface membranes. Exp Cell Res 1984;155:43–49.
52. Wiche G, Krepler R, Artlieb U, Pytela R, Denk H. Occurrence and immunolocalization of plectin in tissues. J Cell Biol 1983; 97:887–901.

Arch Dermatol Res (2007) 298:403–407
DOI 10.1007/s00403-006-0702-0

SHORT COMMUNICATION

N-Linked neutral oligosaccharides in the stratum corneum of normal and ichthyotic skin

Hiroko Ito · Masashi Akiyama · Hiroaki Nakagawa · Rie Uematsu · Kisaburo Deguchi · James R. McMillan · Shin-Ichiro Nishimura · Hiroshi Shimizu

Received: 1 May 2006 / Revised: 23 August 2006 / Accepted: 28 August 2006 / Published online: 26 September 2006

Abstract *N*-Glycan oligosaccharides are thought to play multiple, important roles in a variety of biological events. However, *N*-glycan profiles in the stratum corneum of human skin have not yet been studied in detail. To clarify the *N*-glycan profiles in the stratum corneum of normal and ichthyotic epidermis, *N*-glycan profiles were studied by high-performance liquid chromatography using normal human epidermal samples and scales from hyperkeratotic skin of ichthyosis patients. Chromatograms of patient scale samples showed unique alterations in three peaks eluted at 15.8, 18.8 and 26.9 min. The *N*-glycan profiles were significantly altered in ichthyotic hyperkeratotic skin compared with normal non-hyperkeratotic controls. These findings indicate the reduction of *N*-acetylglucosaminyltransferase II and fucosyltransferase 8 activities. Alteration of *N*-glycan structures in hyperkeratotic skin suggests the biological role of *N*-glycans in keratinization.

Keywords High-performance liquid chromatography · Hyperkeratosis · Neutral oligosaccharide · *N*-Glycan · Oligosaccharide

H. Ito · M. Akiyama (✉) · J. R. McMillan · H. Shimizu
Department of Dermatology,
Hokkaido University Graduate School of Medicine,
North 15 West 7, Sapporo, 060-8638, Japan
e-mail: akiyama@med.hokudai.ac.jp

H. Nakagawa · R. Uematsu · K. Deguchi · S.-I. Nishimura
Division of Biological Sciences,
Frontier Research Center for Post-Genomic Science and Technology,
Hokkaido University Graduate School of Science,
Sapporo, Japan

R. Uematsu
Research Laboratory, Kanebo Cosmetics Inc.,
Odawara, Japan

J. R. McMillan
Creative Research Initiative Sousei,
Hokkaido University, Sapporo, Japan

Oligosaccharides are known to play important roles in a variety of biological events including cell–cell interactions and undergo modifications during cell differentiation [6]. *N*-Glycan oligosaccharides, which bind to asparagine, are a frequent post-translational modification of proteins. *N*-Glycan oligosaccharides exhibit diversity created by sugar linkages and components including: mannose, galactose, *N*-acetylglucosamine, *N*-acetylneuraminic acid. *N*-Glycan oligosaccharides modify specific protein properties, especially glycoprotein localization, secretion and degradation rates of proteins. Alterations in *N*-glycan composition have been reported in many human diseases [6, 12]. Oligosaccharide analyses using oligosaccharide-specific lectins and antibodies have suggested the biological importance of oligosaccharides in the epidermis [3, 5, 7, 19–21, 25, 28]. However, oligosaccharide-specific lectins and antibodies recognize only two or three sugar residues at most and little information has been obtained from studies with lectins or antibodies concerning the entire range of glycan structures or the *N*-glycan and *O*-glycan composition on glycoproteins and glycolipids. The cellular biosynthesis of *N*-glycan is highly regulated and glycan structures significantly affect protein properties [6, 15]. Alteration of *N*-glycan profiles in diseases have

been reported in many human disorders, and these have been used for disease diagnosis and for the elucidation of disease pathomechanisms [4, 8]. Focusing on glycoproteins *N*-glycans, it was demonstrated that the mouse epidermis had abundant high-mannose oligosaccharides [24]. In addition, the oligosaccharide-binding proteins were also determined [24]. However, there are no reports of studies on *N*-glycans in human epidermis. In the present study, we studied *N*-glycan profiles in normal human epidermis and the stratum corneum of ichthyotic, hyperkeratotic skin. *N*-Glycans were specifically released by *N*-glycosidase F and were labeled by pyridylamination with a fluorescence tag. Oligosaccharide profiles were analyzed using high-performance liquid chromatography (HPLC) [10, 22].

Skin samples of normal, non-hyperkeratotic epidermis were collected from control non-palmoplantar skin of three patients with benign skin tumors at resection operations. Skin scale samples were collected from hyperkeratotic skin from the legs of five ichthyosis patients, three non-bullous congenital ichthyosiform erythroderma patients and two lamellar ichthyosis patients. The medical ethical committee at Hokkaido University approved all the described studies. All the participants or parents of the participants gave their written informed consent.

Skin scales were collected by gently scraping the patients' legs with a dull scalpel and stored at −70°C. Normal epidermal samples were obtained at resection operations of benign subcutaneous tumors after obtaining fully informed consent from the patients. Samples from both the ichthyosis patients and normal healthy controls were stored at −70°C.

Normal skin samples were heated to 60°C for 1 min in phosphate buffered saline (PBS) and then cooled on ice. The epidermis was stripped off with a scalpel and was used for further analysis. The epidermis of normal skin samples was washed three times in PBS. Both the scales and the separated epidermis were denatured at 90°C for 10 min in 100 mM NH_4HCO_3 and then finely shredded with scissors.

To degrease the samples, each sample was put into a mixture of chloroform and methanol 2:1 (v/v) 600 µl, mixed well and centrifuged at 3,500 rpm, 4°C for 10 min. Then, the lower layer was removed. This procedure was repeated twice to remove lipids. Organic solvents in the upper layer were vaporized with nitrogen flow at 80°C and the aqueous solution dried in a centrifugal evaporator.

For trypsin and chymotrypsin digestion, the dried samples were suspended in 5 mg per 100 µl of 45 mM Tris–HCl buffer pH 8 containing 10 mM $CaCl_2$, and 0.1 mg trypsin and 0.1 mg chymotrypsin (Sigma-Aldrich Japan, Tokyo, Japan) were added in a 1.5-ml microcentrifuge tube (Eppendorf type). The pH of the solutions was confirmed to be between 7 and 8 by the pH test paper. Toluene was added to the surface of the sample solution and kept at 37°C overnight in an incubator.

For *N*-glycosidase F digestion, trypsin and chymotrypsin were deactivated by heating sample tubes at 90°C for 10 min in a heat block. *N*-Glycosidase F (Roche Diagnostics, Tokyo, Japan) was added, 10 U for each 5 mg sample. The pH of the sample solutions was again confirmed and toluene was added. The samples were kept at 37°C overnight.

Pronase (0.1 mg, Calbiochem, San Diego, CA, USA) was added to each 5 mg of the sample for pronase digestion. pH of the sample solutions was checked again and toluene was added. The samples were incubated at 37°C overnight. After incubation, pronase was deactivated at 90°C for 10 min.

The oligosaccharide fraction was purified by gel-filtration on Bio-gel P-4 (Bio-Rad Laboratories, Hercules, CA, USA) column (1.0 cm × 38 cm) using water as an eluate, and lyophilized completely. The carbohydrates were reductively aminated with 2-aminopyridine and sodium cyanoborohydride [10, 29]. Pyridylaminated (PA)-oligosaccharides were separated from excess reagents by another gel-filtration column step using Sephadex G-15 (GE Healthcare Bioscience Corp., Piscataway, NJ, USA) and 10 mM NH_4HCO_3 and lyophilized again.

Each PA-oligosaccharide was dissolved in 100 µl of 0.01 N HCl and the pH was adjusted to 2 with 0.1 N HCl checking by test paper. PA-oligosaccharide solutions were heated at 90°C for 60 min to remove sialic acids and neutralized with 100 µl of 1 M NH_4HCO_3.

Each PA-oligosaccharide solution was purified by HPLC on an amide–silica column (TSKgel Amide-80 4.6 mm × 250 mm, Tosoh Corporation, Tokyo, Japan) using two solvents, A and B, at a flow rate of 1.0 ml/min at 40°C. Solvent A comprised 65% (v/v) of acetonitrile and 35% of 0.5 M acetic acid–triethylamine buffer pH 7.3 and solvent B was 35 and 65%, respectively. The column was equilibrated only with solvent A and 7 min after injection of each sample, the flow was changed to solvent B only. The *N*-glycan fraction that eluted between 8 and 12 min was collected and centrifugally evaporated.

Each oligosaccharide mixture was dissolved in water and analyzed by HPLC using the previously described procedure [22]. The PA-oligosaccharide mixture was applied on an ODS column (HRC-ODS 6 mm × 150 mm, Shimadzu Corporation, Kyoto, Japan). The

column was equilibrated with 0.1% (v/v) 1-butanol in 10 mM sodium phosphate buffer pH 3.8 and concentration of 1-butanol was linearly increased to 0.25% in 60 min. The flow rate was 1.0 ml/min and the column was controlled at 55°C. PA-glycans were detected by fluorescence, excitation at 320 nm and emission at 400 nm.

N-Glycan profiles from the patients and normal control epidermis are shown in Fig. 1 as chromatograms on an ODS column. *N*-Glycan eluted after 5 min and few contamination peaks were detected in this region. High-mannose type *N*-glycans eluted from 5 to 10 min and complex-type and hybrid-type *N*-glycans appeared at 10 min or later in this analysis. Three peaks, a, b and c, eluted at 15.8, 18.8 and 26.9 min, respectively, and these profiles were significantly altered in ichthyotic skin. The rates of these peaks are shown in Fig. 2. Peak c significantly decreased and peak b increased in the ichthyotic skin compared with normal controls. Peak a was also larger in the patients, but the statistical change in this level was not significant. Using two-dimensional mapping [22], peaks a, b and c to corresponded to major serum *N*-glycans, Galβ1,4GlcNAcβ1,2Manα1, 3(Galβ1,4GlcNAcβ1,2Manα1,6)Manβ1,4GlcNAcβ1,4 GlcNAc,Galβ1,4GlcNAcβ1,2Manα1,3(Manα1,6)Man β1,4GlcNAcβ1,4(Fucα1,6)GlcNAc and Galβ1,4GlcN Acβ1,2Manα1,3(Galβ1,4GlcNAcβ1,2Manα1,6)Manβ 1,4GlcNAcβ1,4(Fucα1,6)GlcNAc, respectively [17, 22].

Changes in *N*-glycan oligosaccharides have mainly been reported in carcinomas in the course of progression or during metastatic change [13, 14, 23]. In the epidermis, glycoconjugate profile changes were studied by lectin histochemistry in a variety of skin diseases [1, 2, 9]. In several autoimmune skin diseases, autoantibody targets have been shown to be *N*-linked oligosaccharides [18]. However, to our knowledge, this is the

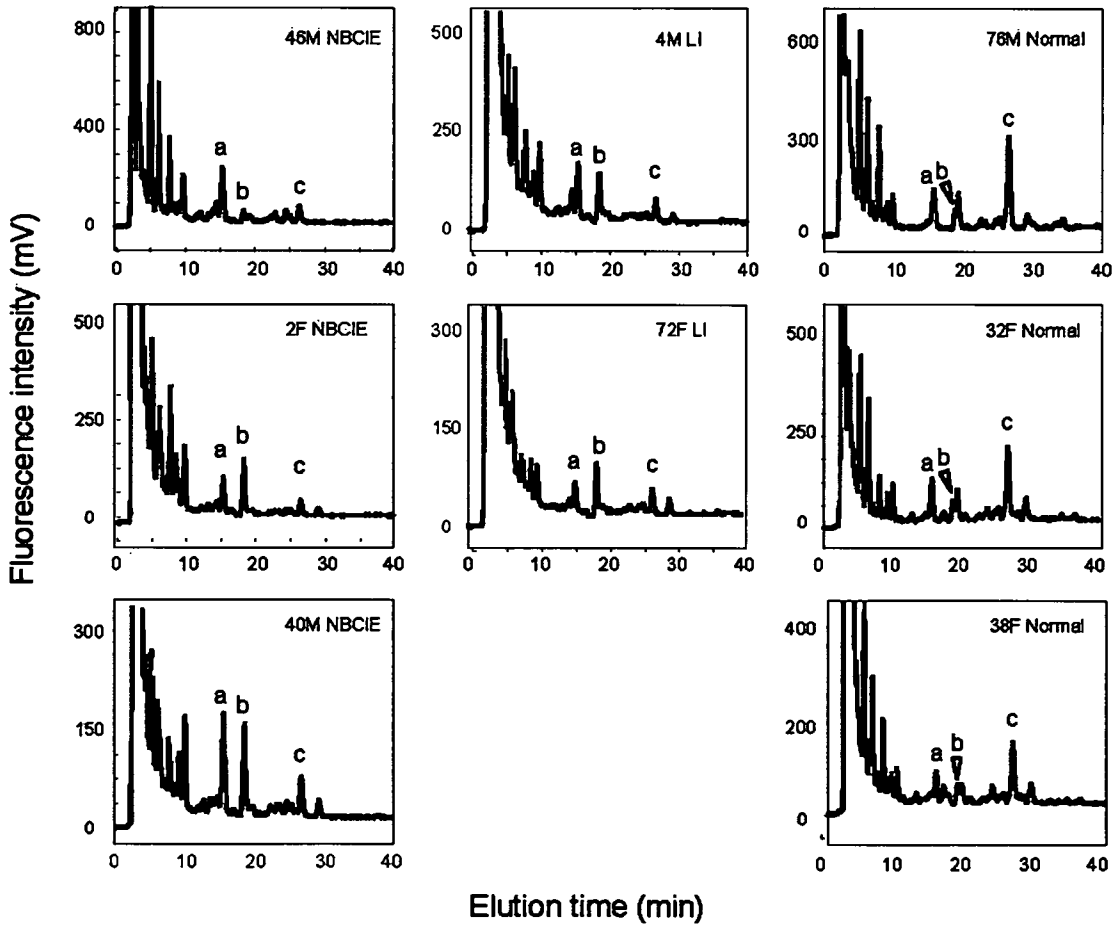

Fig. 1 Chromatograms of *N*-glycans from the epidermis. Fluorescence-tagged glycans released from the epidermis of patients and normal controls on an ODS column using HPLC. Peaks *a*, *b* and *c* correspond to *N*-glycans, Galβ1,4GlcNAcβ1,2Manα1,3 (Galβ1,4GlcNAcβ1,2Manα1,6)Manβ1,4GlcNAcβ1,4GlcNAc,Galβ1,4GlcNAcβ1,2Manα1,3(Manα1,6)Manβ1,4GlcNAcβ1,4(Fucα1, 6)GlcNAc and Galβ1,4GlcNAcβ1,2Manα1,3(Galβ1,4GlcNAcβ1, 2Manα1,6)Manβ1,4GlcNAcβ1,4(Fucα1,6)GlcNAc, respectively. *LI* lamellar ichthyosis, *NBCIE* non-bullons congenital ichthyosiform erythroderma

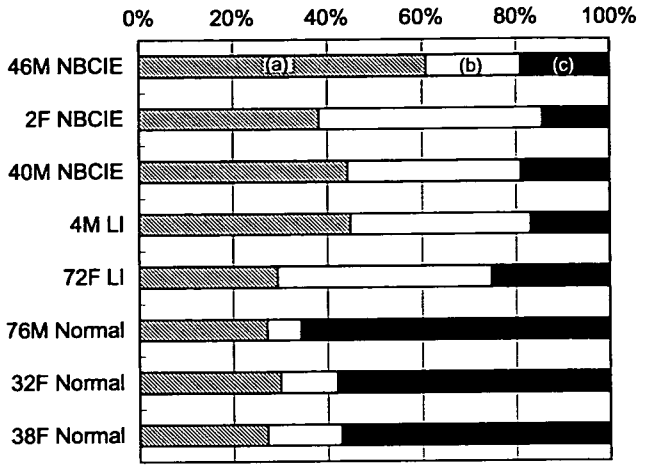

Fig. 2 Rates of molecular compartments, *a*, *b* and *c*. Compartments *a* and *b* were increased and compartment *c* decreased in the hyperkeratotic diseased skin from patients. Colors of *bar* show following: slashed, a; white, b; black c; *LI* lamellar ichthyosis, *NBCIE* non-bullons congenital ichthyosiform erythroderma

first study that reported *N*-linked oligosaccharide profiles in normal and hyperkeratotic epidermis.

Glycosylation is the major post-translational modification of many proteins. The *N*-Glycan precursor, Glc3Man9GlcNAc2, is introduced to asparagine residues of Asn-X-Ser/Thr sequence while polypeptide synthesis occurs in the endoplasmic reticulum. The Glc residues are removed while protein holding occurs. High-mannose type *N*-glycans work as a tag in the transfer of a protein folded correctly to the Golgi apparatus or misfolded one to degradation system [11]. In the Golgi apparatus, several enzymes modify *N*-glycan oligosaccharides from the high-mannose type into a more complex type by trimming and repetitive addition of sugar residues [15]. The biosynthesis of *N*-glycans is highly conserved and these oligosaccharide residues on proteins have important roles in promoting protein regulation, folding, quality control, sorting and transport [6].

The *N*-glycan alterations seen in ichthyotic skin failed to suggest novel oligosaccharide structures, although the rates of known oligosaccharide structures were changed. Peak a is the most common *N*-glycan in the human serum. Peak b is formed due to insufficient activity of *N*-acetylglucosaminyltransferase II (GnT-II) and peak c is produced from peak a *N*-glycan by fucosyltransferase 8 (Fut8) activity [6]. The GnT-II knock-out mice were reported to die from serious defects of multiple organs in early postnatal development, mainly from abnormalities in the gastrointestinal tracts, hematopoietic systems and bones, although skin involvements were not apparent [26]. The Fut8 null mice were also lethal in early postnatal days mainly from emphysema-like changes in the lung [27]. The Fut8 null mice were known to overexpress matrix metaloproteinases and to show function loss of TGF-β receptor. TGF-β mediates a variety of signaling pathways [16] and dysfunction of TGF-β receptor may be associated with skin symptoms of ichthyosis in the present study. On the other hand, there is a possibility that disturbed differentiation of epidermal keratinocytes resulted in the altered *N*-glycan profiles in the ichthyotic lesions. In any case, the relationship between *N*-glycan alteration and hyperkeratosis is an interesting finding that may help to clarify the pathomechanism(s) of hyperkeratosis.

Epidermal proteins, which comprise high levels of mannose-type oligosaccharides, were analyzed in mouse [24]. These high-mannose type oligosaccharides are located in lysosomes, lamellar granules and cell–cell connection desmosome sites. Desmocollins and desmogleins are also assigned as carriers of high-mannose type oligosaccharides, and it was suggested that high-mannose type oligosaccharides control desquamation [24]. However, in the present samples of hyperkeratotic skin, the profile of the high-mannose type oligosaccharides was not changed. These results indicated that *N*-glycans bound to cell surface proteins were more seriously affected than those in the cytoplasm and desmosomes. Further studies into *N*-glycan structures and the respective proteins carrying the *N*-glycans in hyperkeratotic skin will provide further clues to determine the exact mechanisms that lead to hyperkeratosis in human skin.

Acknowledgments The authors thank Ms Mayuko Nagasaki for her excellent technical assistance. This work was partly supported by a grant for the National Project on "Functional Glycoconjugate Research Aimed at Developing New Industry" from the Ministry of Education, Science, Sport and Culture of Japan.

References

1. Akiyama M, Hayakawa K, Watanabe Y, Nishikawa T (1990) Lectin-binding sites in clear cell acanthoma. J Cutan Pathol 17:197–201
2. Akiyama M, Sugiura M, Shimizu H, Nishikawa T (1991) No significant change of glycoconjugates exists in the epidermis of familial benign chronic pemphigus. Arch Dermatol Res 283:537–539
3. Bell CM, Skerrow CJ (1984) Factors affecting the binding of lectins to normal human skin. Br J Dermatol 111:517–526
4. Butler M, Quelhas D, Critchley AJ, Carchon H, Hebestreit HF, Hibbert RG, Vilarinho L, Teles E, Matthijs G, Schollen E, Argibay P, Harvey DJ, Dwek RA, Jaeken J, Rudd PM (2003) Detailed glycan analysis of serum glycoproteins of patients with congenital disorders of glycosylation indicates the specific defective glycan processing step and provides an insight into pathogenesis. Glycobiology 13:601–622

5. Dabelsteen E, Buschard K, Hakomori S-I, Young WW (1989) Pattern of distribution of blood group antigens on human epidermal cells during maturation. J Invest Dermatol 82:13–17
6. Dwek RA (1996) Glycobiology: toward understanding the function of sugars. Chem Rev 96:683–720
7. Elias PM, Chung JC, Orozco-Topete R, Nemanic MK (1983) Membrane glycoconjugate visualization and biosynthesis in normal and retinoid-treated epidermis. J Invest Dermatol 81:81s–85s
8. Fukuda MN, Dell A, Scartezzini P (1987) Primary defect of congenital dyserythropoietic anemia type II. J Biol Chem 262:7195–7206
9. Gheri G, Russo G, Cappugi P, Sgambati E, Bryk SG (1999) The oligosaccharidic component of the glycoconjugates in lichen planus, granuloma annulare, seborrheic keratosis and plamoplantar keratoderma: lectin histochemical study. Histol Histopathol 14:697–704
10. Hase S, Ikenaka T, Matsushima Y (1978) Structure analyses of oligosaccharides by tagging of the reducing end sugars with a fluorescent compound. Biochem Biophys Res Commun 85:257–263
11. Helenius A, Aebi M (2001) Intracellular functions of *N*-linked glycans. Science 291:2364–2369
12. Helenius A, Aebi M (2004) Role of *N*-linked glycans in the endoplasmic reticulum. Annu Rev Biochem 73:1019–1049
13. Ishimura H, Takahashi T, Nakagawa H, Nishimura S-I, Hagisawa S, Arai Y, Horikawa Y, Habuchi T, Miyoshi E, Ohyama C (2006) *N*-Acetylglucosaminyltransferase-V (GnT-V) and β 1,6 branching *N*-linked oligosaccharides are associated with good prognosis of the patients with bladder cancer. Clin Cancer Res 102:15791–15796
14. Jorgensen T, Berner A, Kaalhus O, Tveter KJ, Danielsen HE, Bryne M (1995) Up-regulation of the oligosaccharide sialyl LewisX: a new prognostic parameter in metastatic prostate cancer. Cancer Res 55:1817–1819
15. Kornfeld R, Kornfeld S (1985) Assembly of asparagine-linked oligosaccharides. Annu Rev Biochem 54:631–664
16. Massagué J, Blain SW, Lo RS (2000) TGFβ signaling in growth control, cancer, and heritable disorders. Cell 103:295–309
17. Nakagawa H, Kawamura Y, Kato K, Shimada I, Arata Y, Takahashi N (1995) Identification of neutral and sialyl *N*-linked oligosaccharide structures from human serum glycoproteins using three kinds of high-performance liquid chromatography. Anal Biochem 226:130–138
18. Shimanovich I, Hirako Y, Sitaru C, Hashimoto T, Brocker EB, Butt E, Zillikens D (2003) The autoantigen of anti-p200 pemphigoid is an acidic noncollagenous *N*-linked glycoprotein of the cutaneous basement membrane. J Invest Dermatol 121:1402–1408
19. Skerrow CJ, Clelland DG, Skerrow D (1989) Changes to desmosomal antigens and lectin-binding sites during differentiation in normal human epidermis: a quantitative ultrastructural study. J Cell Sci 92:667–677
20. Srikrishna G, Varki NM, Newell PC, Varki A, Freeze HH (1997) An IgG monoclonal antibody against *Dictyostelium discoideum* glycoproteins specifically recognizes Fucα1,6GlcNAcβ in the core of *N*-linked glycans. J Biol Chem 272:25743–25752
21. Symington FW, Holmes EH, Symington BE (1992) Human epidermal keratinocyte expression of sialyl-Lewis X. J Invest Dermatol 99:601–607
22. Tomiya N, Awaya J, Kurono M, Endo S, Arata Y, Takahashi N (1988) Analyses of *N*-linked oligosaccharides using a two-dimensional mapping technique. Anal Biochem 1715:73–90
23. Tsuchiya N, Yamanaka R, Yajima N, Homma J, Sano M, Komata T, Ikeda T, Fujimoto I, Takahashi H, Tanaka R, Ikenaka K (2005) Isolation and characterization of an *N*-linked oligosaccharide that is increased in glioblastoma tissue and cell lines. Int J Oncol 27:1231–1239
24. Uematsu R, Furukawa J-I, Nakagawa H, Shinohara Y, Deguchi K, Monde K, Nishimura S-I (2005) High throughput quantitative glycomics and glycoform-focused proteomics of murine dermis and epidermis. Mol Cell Proteomics 4:1977–1989
25. Virtanen I, Kariniemi A-L, Holthöfer H, Lehto VP (1986) Fluorochrome-coupled lectins reveal distinct cellular domains in human epidermis. J Histochem Cytochem 34:307–315
26. Wang Y, Tan J, Sutton-Smith M, Ditto D, Panico M, Campbell RM, Varki NM, Long JM, Jaeken J, Levinson SR, Wynshaw-Boris A, Morris HR, Le D, Dell A, Schachter H, Marth JD (2001) Modeling human congenital disorder of glycosylation type IIa in the mouse: conservation of asparagine-linked glycan-dependent functions in mammalian physiology and insights into disease pathogenesis. Glycobiology 11:1051–1070
27. Wang X, Inoue S, Gu J, Miyoshi E, Noda K, Li W, Mizuno-Horikawa Y, Nakano M, Asahi M, Takahashi M, Uozumi N, Ihara S, Lee SH, Ikeda Y, Yamaguchi Y, Aze Y, Tomiyama Y, Fujii J, Suzuki K, Kondo A, Shapiro SD, Lopez-Otin C, Kuwaki T, Okabe M, Honke K, Taniguchi N (2005) Dysregulation of TGF-beta1 receptor activation leads to abnormal lung development and emphysema-like phenotype in core fucose-deficient mice. Proc Natl Acad Soc USA 102:15791–15796
28. Watt FM (1983) Involucrin and other markers of keratinocyte terminal differentiation. J Invest Dermatol 81:100s–103s
29. Yamamoto S, Hase S, Fukuda S, Sano O, Ikenaka T (1989) Structures of the sugar chain of interferon-γ produced by human myelomonocyte cell line HBL-38. J Biochem 105:547–555

ORIGINAL ARTICLE

DNA-Based Prenatal Diagnosis of Harlequin Ichthyosis and Characterization of *ABCA12* Mutation Consequences

Masashi Akiyama[1,5], Matthias Titeux[2,5], Kaori Sakai[1], James R. McMillan[1], Laure Tonasso[2], Patrick Calvas[3], Frederique Jossic[4], Alain Hovnanian[2,3] and Hiroshi Shimizu[1]

Until the identification of *ABCA12* as the causative gene, prenatal diagnosis (PD) for harlequin ichthyosis (HI) had been performed by electron microscopic observation of fetal skin biopsy samples. We report the first case of HI DNA-based PD. Direct sequence analysis of *ABCA12* revealed that the deceased proband was a compound heterozygote for two novel mutations. The maternal nonsense mutation p.Ser1249Term likely leads to nonsense-mediated messenger RNA decay. The paternal mutation c.7436G>A affects the last codon of exon 50 and was expected to be a splice site mutation. For their third pregnancy, the parents requested PD. Direct sequence analysis of fetal genomic DNA from amniotic fluid cells at 17 weeks gestation revealed the fetus was a compound heterozygote for both mutations. The parents requested the pregnancy to be terminated. Analysis of *ABCA12* transcripts of cultured keratinocytes from the abortus showed the presence of six abnormally spliced products from the allele carrying the splice site mutation. Four of them lead to premature termination codons whereas the two others produced shortened proteins missing 21 and 31 amino acids from the second ATP-binding cassette. This report provides evidence for residual ABCA12 expression in HI, and demonstrates the efficiency of early DNA-based PD of HI.

Journal of Investigative Dermatology (2007) **127**, 568–573. doi:10.1038/sj.jid.5700617; published online 2 November 2006

INTRODUCTION

Harlequin ichthyosis (HI) is a severe and usually fatal congenital ichthyosis with an autosomal recessive inheritance pattern (Williams and Elias, 1987; Akiyama, 2006). The clinical features include thick, plate-like scales with ectropion, eclabium, and flattened ears. Infants affected with HI frequently die within the first few weeks of life. Skin development is altered *in utero*; hyperkeratosis of the hair canal occurs in the second trimester and characteristic ultrastructural abnormalities including abnormal lamellar granules, are present in the affected fetal epidermis (Dale *et al.*, 1990; Akiyama *et al.*, 1994, 1998). Before the gene underlying HI was identified in 2005, prenatal diagnosis (PD) of the disease relied on ultrastructural examination of fetal skin biopsy samples at 19–23 weeks estimated gestational age (EGA) (Blanchet-Bardon *et al.*, 1983; Suzumori and Kanzaki, 1991; Akiyama *et al.*, 1994, 1999).

ABCA12 is a transporter which belongs to the ATP-binding cassette (ABC) transporter superfamily (Annilo *et al.*, 2002; Uitto, 2005). In 2005, we identified serious loss of function mutations in *ABCA12* coding an ABC transporter, that leads to defective lipid transport in epidermal keratinocytes and results in an HI phenotype (Akiyama *et al.*, 2005). Another group independently demonstrated that mutations in ABCA12 underlie HI by linkage analysis (Kelsell *et al.*, 2005). Thus, HI PD using molecular *ABCA12* mutational analysis has become possible. We report here the first successful DNA-based PD for HI using fetal genomic DNA specimens from amniotic fluid cells.

RESULTS

Case history and the clinical features of the proband

The newborn proband was the first child from unrelated, healthy French parents. He was affected with HI and died soon after birth. He displayed severe hyperkeratosis with fissures over his entire body, severe ectropion, and eclabium (Figure 1a–c). There was no family history of genodermatoses in the family. The parents had a healthy son, their second child. For their third pregnancy, the parents requested HI PD.

[1]*Department of Dermatology, Hokkaido University Graduate School of Medicine, Sapporo, Japan;* [2]*Inserm, U563 and University Paul Sabatier, Toulouse, France;* [3]*Department of Medical Genetics, Purpan Hospital, Toulouse, France and* [4]*Department of Fetopathology, Nantes Hospital, Nantes, France*

[5]*These authors contributed equally to this work*

Correspondence: Dr Masashi Akiyama, Department of Dermatology, Hokkaido University Graduate School of Medicine, North 15 West 7, Kita-ku, Sapporo 060-8638, Japan. E-mail: akiyama@med.hokudai.ac.jp

Abbreviations: ABC, ATP-binding cassette; cDNA, complementary DNA; EGA, estimated gestational age; HI, harlequin ichthyosis; HIK, HI keratinocytes; LG, lamellar granule; mRNA, messenger RNA; NHK, normal human keratinocytes; PD, prenatal diagnosis

Received 20 June 2006; revised 18 August 2006; accepted 19 September 2006; published online 2 November 2006

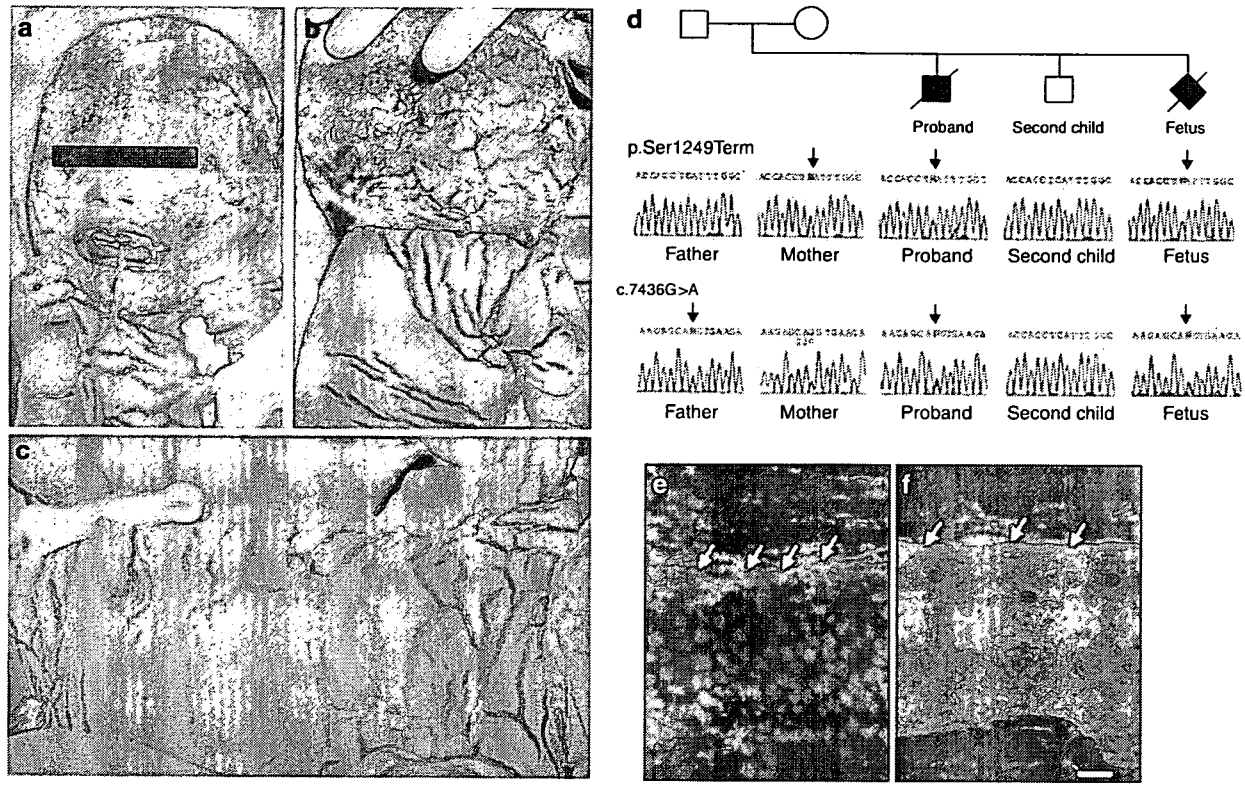

Figure 1. Clinical features of the proband, ABCA12 mutations in the family, and abnormal ABCA12 immunostaining in the patient's epidermis. (**a**, **b**, and **c**) Severe hyperkeratosis with fissures covering (**a**) the proband's face (**b**) scalp and back, (**c**) chest and abdomen. (**a**) Eclabium and (**b**) malformed pinna were apparent. (**d**) A novel nonsense mutation p.Ser1249Term was found in the proband, the mother, and the fetus (arrows). The novel splice site mutation c.7436G>A was detected in the proband, the father and the fetus (arrows). The fetus was prenatally diagnosed as affected. (**e**) In the patient's upper epidermis, weak ABCA12 immunostaining (green: arrows) was seen diffusely in the keratinocyte cytoplasm. (**f**) In normal control human epidermis, intense ABCA12 labeling (green) was noted in the granular layers (arrows). ABCA12, FITC (green); nuclear staining, propidium iodide (red). Bar = 10 μm.

ABCA12 mutation analysis

Mutation analysis of the 53 exons including the intron–exon boundaries of the entire *ABCA12* gene revealed that the proband was a compound heterozygote for two novel *ABCA12* mutations, c.3746C>A and c.7436G>A (sequence according to Lefèvre *et al.* (2003)) (GenBank accession NM 173076) (Figure 1d). c.3746C>A in exon 26 was a novel nonsense mutation that changed a serine residue at codon 1249 to a stop codon (p.Ser1249Term). This nonsense mutation p.Ser1249Term in exon 26 likely leads to nonsense-mediated messenger RNA (mRNA) decay rather than protein truncation, resulting in ABCA12 deficiency (see section *ABCA12* transcript analysis in cultured keratinocytes from the fetus). The mutation p.Ser1249Term was also found in the mother. The other mutation c.7436G>A in exon 50 affects the last amino acid of exon 50 and was expected to be a splice site mutation. Its potential effects on the splicing pattern of *ABCA12* pre-mRNA were investigated (see section *ABCA12* transcript analysis in cultured keratinocytes from the fetus). This splice site mutation was found in the father. Thus, the nonsense mutation p.Ser1249Term was of maternal origin and the splice site mutation c.7436G>A of paternal origin. These mutations were not found in 200 normal alleles (50 French and 50 Japanese healthy unrelated individuals) by sequence analysis, and were unlikely to be polymorphic variations (data not shown).

DNA-based PD of the fetus

Direct sequencing of PCR products including exon 26 or 50 of *ABCA12* from the fetal genomic DNA revealed the presence of the maternal nonsense mutation p.Ser1249Term in exon 26 and the paternal splice site mutation c.7436G>A in exon 50 (Figure 1d). Thus, the fetus harbored both *ABCA12* pathogenic mutations and was predicted to be affected. The pregnancy was terminated at 19 weeks gestation after the parents' request. The fetus showed characteristic changes including thin and fragile skin with petechia, eclabium, small, thickened and abnormally rimmed ears, rigid and swollen fingers and toes.

ABCA12 protein expression in the proband's skin

In the patient, ABCA12 immunostaining in the upper epidermis was reduced (Figure 1e), when compared with the intense ABCA12 immunostaining in the upper epidermal layers, mainly in the granular layers, of normal human skin (Figure 1f).

Ultrastructure of the skin from the abortus

Autopsy skin samples from the abortus showed abnormal, vacuolated lamellar granules in the upper intermediate cells and a large number of lipid droplets in the cytoplasm of incompletely keratinized keratinocytes.

ABCA12 transcript analysis in cultured keratinocytes from the fetus

Analysis of reverse transcription-PCR products from cultured keratinocytes of the fetus HI keratinocyte (HIK) and normal human keratinocytes (NHKs) on agarose gel electrophoresis revealed the presence of a single band in NHK PCR products and three bands in HIK PCR products (data not shown). PCR products were subsequently cloned and sequenced. A total of seven different mRNAs generated from the allele carrying the c.7436G>A mutation were identified (Figure 2a and b). Transcript p.Arg2479Lys corresponds to the full-length *ABCA12* transcript carrying a lysine residue in place of the arginine 2479. In addition, six of these transcripts are generated by splicing from several cryptic splice donor sites located in exon 50 of *ABCA12*. Transcript Δ4 carries a 4 bp deletion around the mutation (c.7433_7436del) leading to a frameshift and a PTC 11 amino acids downstream (p.Arg2479Leufs × 11). Transcript Δ31 displays a 31 bp deletion (c.7406_7436del) leading to a frameshift and a PTC 11 downstream (p.Ile2470_Arg2479>Leufs × 11). Transcript Δ43 presents a 43 bp deletion (c.7394_7436del) leading to a frameshift and a PTC 11 amino acids downstream (p.Lys2466_Arg2479>Leufs × 11). Transcript Δ50 shows a 50 bp deletion (c.7387_7436del) leading to a frameshift and a PTC 13 amino acids downstream (p.Asn2464_Arg2479>Trpfs × 13). Interestingly, transcript Δ63 predicts a truncated protein deleted from Leucine 2459 to Arginine 2479 (p.Leu2459_Arg2479del) owing to an in

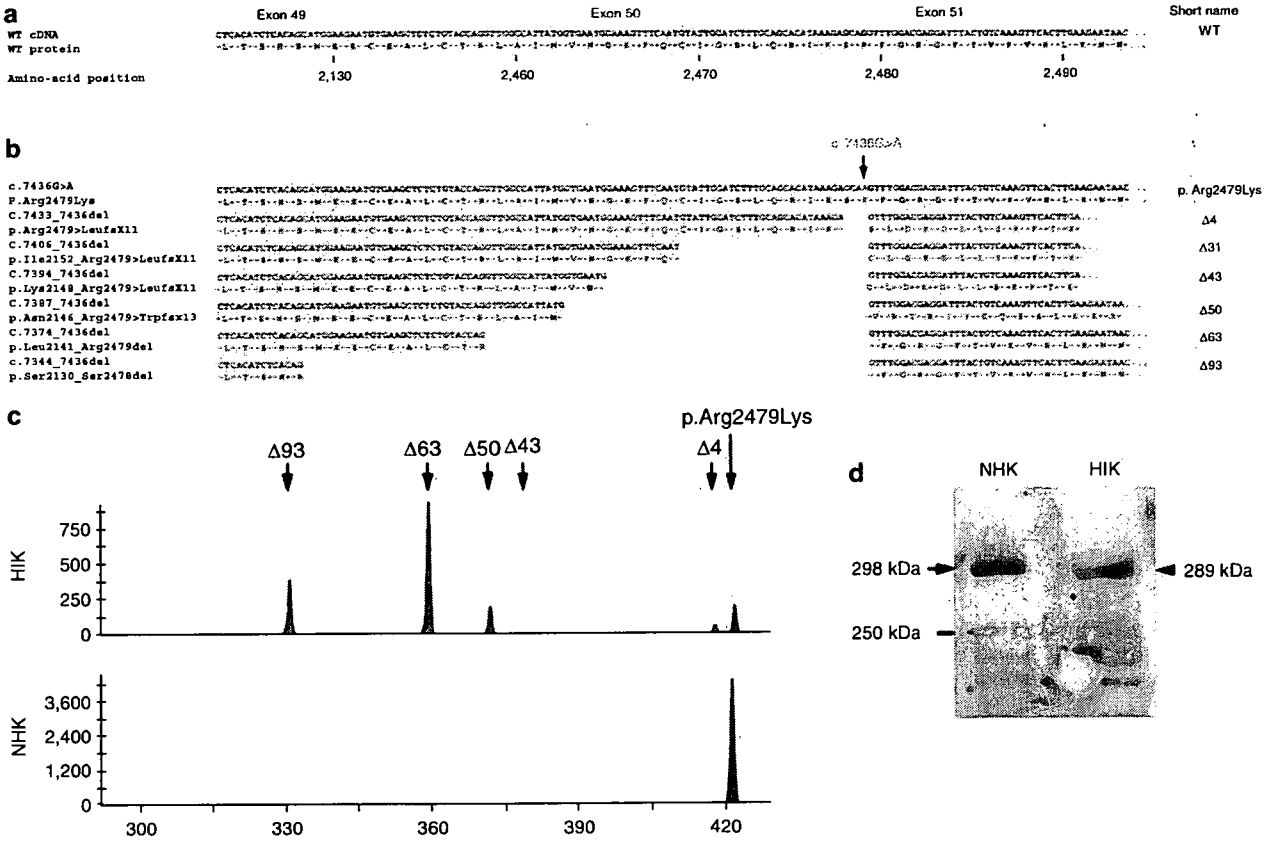

Figure 2. Expression analysis of ABCA12 transcripts and protein. (**a** and **b**) Sequence alignment of the several transcripts generated by the allele carrying the paternal splice site mutation c.7436G>A. (**a**) Wild-type cDNA (blue) and protein sequences of exon 50 of *ABCA12*. Amino-acid numbering is indicated. (**b**) Nucleotide and deduced protein sequences of splice variants of the allele carrying the c.7436G>A mutation (green). Premature stop codons and aberrant sequences owing to frameshifts are indicated in red. Splice variants include the correctly spliced product (p.Arg2479Lys) and six aberrantly spliced forms leading to out-of-frame (transcripts Δ4, Δ31, Δ43, and Δ50) and in-frame (Δ63 and Δ93) deletions. (**c**) Capillary electrophoresis analysis of *ABCA12* cDNA amplimers. Fragments extending over exons 49–53 were amplified by PCR using reverse-transcribed mRNA from primary cultures of HIK and NHKs. Although only one peak at 422 bp is present in NHK, several peaks are detected in HIK. The peak at 422 bp corresponds to the full-length transcript, arising either from the wild-type alleles (in NHK) or from the allele carrying the p.Ser1249Term null mutation and from the allele carrying the p.Arg2479Lys mutation (in HIK). The other peaks at 418, 379, 372, 359, and 329 bp, correspond respectively to transcripts Δ4, Δ43, Δ50, Δ63, and Δ93. The relative amount of each transcript, evaluated by the size of the peaks, shows that transcript Δ63 is predominant. Note that transcript Δ31 is missing, probably because its synthesis level is below the detection threshold of this technique. (**d**) Western blot analysis of ABCA12 protein in NHK and in HIK. A band at 298 kDa (arrow) is present in NHKs extract, however a slightly lower band (arrowhead, 289 kDa) is present in the HIK extracts. This lower band probably arises from the transcript Δ63 and to a less extent from the transcript Δ93.

frame deletion of 63 bp (c.7374_7436del), whereas transcript Δ93 presents an in frame skipping of the entire exon 50 predicting a truncated protein deleted from Serine 2448 to Serine 2478 (p.Ser2448_Ser2478del). The cryptic splice sites used to generate transcripts Δ4, Δ31, Δ50, and Δ63 were predicted using the automated splice site analysis software by Nalla and Rogan (2005).

Capillary electrophoresis analysis of the *ABCA12* complementary DNA (cDNA) amplimers showed one amplimer (422 bp) in NHKs corresponding to the normal sequence of exon 50, whereas five abnormal species were present in HIK (Figure 2c). All but one (Δ31) identified transcripts were found. The relative amount of transcript, indicated by the height of the peaks, showed that the Δ63 transcript is predominant, whereas the Δ31 transcript was not detectable. Interestingly, the height of the peak at 422 bp which arises from both the p.Arg2479Lys transcript and from the transcript synthesized from the other *ABCA12* allele carrying the p.Ser1249Term mutation is weak, indicating that the amount of both transcripts is low. This suggests that the allele carrying the null mutation is likely to be subjected to nonsense mediated mRNA decay and that only a small amount of ABCA12 protein arise from the natural splice site of the pre-mRNA carrying the c.7436G>A.

ABCA12 protein expression in fetal cultured keratinocytes

Western blot analysis revealed the presence of a band of an expected molecular weight of 298 kDa in protein extracts from NHKs, whereas a slightly smaller band of 289 kDa was seen in HI keratinocyte extracts (Figure 2d). This band probably corresponds to the proteins synthesized from both transcript Δ63 and transcript Δ93 which are predicted to encode proteins of calculated molecular weight of 291 and 289 kDa, respectively, and cannot be resolved on the SDS-PAGE. Smaller bands were seen in both extracts and probably correspond to degradation products. Western blot analysis failed to reveal the presence of other shortened proteins in the extract of HIK. However, the epitope recognized by the antibody is located at the end of the C-terminus domain of ABCA12 and thus is not present in the predicted proteins encoded by transcripts Δ4, Δ31, Δ43, and Δ50, and by the product of the allele carrying the p.Ser1249Term mutation.

DISCUSSION

HI is the most severe ichthyotic genodermatosis and has a very poor prognosis. Therefore, any parents' request for PD should be taken very seriously. However, until 2005 the causative gene had not been identified and previous prenatal diagnoses were performed using electron microscopic examination of fetal skin biopsies during the later stages of pregnancies (Blanchet-Bardon *et al.*, 1983; Suzumori and Kanzaki, 1991; Akiyama *et al.*, 1994, 1999). HI PD by fetal skin biopsy was usually performed at 21–22 weeks EGA (Blanchet-Bardon *et al.*, 1983; Suzumori and Kanzaki, 1991; Akiyama *et al.*, 1994, 1999). According to these reports, fetal skin biopsy specimens at that age showed characteristic abnormalities including a large number of lipid droplets in the keratinized cells and abnormal or absent lamellar granules, which were sufficient findings for the PD of the disorder.

However, PD of HI by fetal skin biopsy is technically difficult, requires excellent skin biopsy site selection, and is time-consuming. We need to gain a significant better understanding of fetal skin development and only a few experts are able to make this reliable diagnosis. Owing to the fact that the interfollicular epidermis at 19 weeks EGA or earlier is not sufficiently developed to exhibit the characteristic morphologic changes of keratinization (Holbrook and Odland, 1980), the observations of interfollicular keratinocytes are thought to sometime provide insufficient or unreliable information for PD or prenatal exclusion of HI. However, at 19 weeks EGA, we were able to see characteristic ultrastructural HI abnormalities in the keratinized cells in the hair canal or infundibulum of the developing hair follicle in the case of an affected fetus (Akiyama *et al.*, 1999). This is because keratinization in the hair cone and hair canal occurs at around 15 weeks EGA, approximately 8–9 weeks before the keratinization of interfollicular epidermis in human fetal skin development (Holbrook and Odland, 1978). However, fetal biopsy specimens at 19 weeks EGA may not always provide sufficient information for PD or exclusion of HI because the interfollicular epidermis has not yet keratinized at this stage of epidermal development (Shimizu *et al.*, 2005).

In 2005, *ABCA12* was identified as the underlying gene causing HI (Akiyama *et al.*, 2005; Kelsell *et al.*, 2005). Additional HI cases harboring *ABCA12* mutations have now been reported (Akiyama *et al.*, 2006a, b). Owing to these discoveries, it has now become possible to undertake HI DNA-based PD by chorionic villus or amniotic fluid sampling from the earlier stages of pregnancy. These procedures are technically more reliable and have a reduced burden on the mothers, as in other severe genetic keratinization disorders (Tsuji-Abe *et al.*, 2004). We report here a successful PD of HI using fetal genomic DNA obtained at 17 weeks EGA. It is anticipated that in the future, even earlier prenatal diagnoses using completely non-invasive analysis of DNA from fetal cells in the maternal circulation will be possible (Uitto *et al.*, 2003), as well as pre-implantation genetic diagnosis for HI (Shimizu and Suzumori, 1999).

Expression analysis of *ABCA12* in cultured keratinoctyes from the abortus revealed that the allele carrying the c.7436G>A mutation produced seven different transcripts. The synthesis of six different truncated or deleted transcripts from this allele explains the loss of function of this allele. In particular, transcripts Δ63 and Δ93 predict the synthesis of deleted proteins (deletion of 21 and 31 amino-acid residues, respectively) with calculated molecular weights of 291 and 289 kDa, which cannot be separated on the SDS-PAGE. Thus, the protein detected at 289 kDa is likely to arise from both transcripts, but predominantly from transcript Δ63, which is present in higher amount. The two proteins lack part of the second ATP-binding cassette, which is predicted to dramatically affect ABCA12 function. Although, small amounts of a full-length ABCA12 protein carrying the p.Arg2479Lys mutation may theoretically be synthesized, they were not

detected. Thus, loss of ABCA12 function results from the combination of a null allele, and the synthesis of non-functional deleted proteins unable to restore a normal phenotype.

The terminated fetuses in the previous reports of positive PD of HI showed macroscopic changes consistent with the HI phenotype at 22 weeks or older EGA (Blanchet-Bardon *et al.*, 1983; Suzumori and Kanzaki, 1991; Akiyama *et al.*, 1994, 1999). In our previous report, we demonstrated that an affected fetus already showed a clinically apparent HI phenotype at 21 weeks EGA (Akiyama *et al.*, 1999). Characteristic HI changes of HI were seen both macroscopically and ultrastructurally at 19 weeks EGA and the present case suggests that the HI phenotype has started to emerge in the affected fetus at the late second trimester of pregnancy.

MATERIALS AND METHODS

Mutation detection

Mutational analysis was performed in the proband and both parents. Briefly, genomic DNA isolated from peripheral blood was subjected to PCR amplification, followed by direct automated sequencing using an ABI PRISM 3100 genetic analyzer (ABI Advanced Biotechnologies, Columbia, MD). Oligonucleotide primers and PCR conditions used for amplification of all exons 1–53 of *ABCA12* were originally derived from the report by Lefèvre *et al.* (2003) and were partially modified as described previously (Akiyama *et al.*, 2005). The entire coding region including the exon/intron boundaries for both forward and reverse strands from the proband, the parents and 100 healthy control individuals (50 French and 50 Japanese) were sequenced.

DNA-based prenatal testing

Amniotic fluid cells were obtained under ultrasound guidance at 17 weeks gestation. Fetal DNA was extracted from fresh cells, and detection of *ABCA12* mutations targeting the mutations that were found in the proband was subsequently performed, as described above. There were no sonographic findings suggestive of an affected fetus. No complications arose from the procedure.

Cell culture

Primary human keratinocytes and fibroblasts were obtained from skin fragments of the abortus and a punch biopsy of a healthy control. Keratinocytes were cultured on a feeder layer of lethaly irradiated mouse 3T3-J2 fibroblasts as described previously (Barrandon and Green, 1987). Fibroblasts were grown in DMEM supplemented with 10% heat-inactivated fetal calf serum (Eurobio, Les Ulis, France).

RNA extraction and reverse transcription-PCR analysis

RNA from cultured keratinocytes and fibroblasts was extracted with the SV Total RNA Isolation System (Promega, Charbonnières, France), and first-strand cDNA synthesis was carried out using random hexamer primers and superscript II reverse transcriptase (Invitrogen, Carlsbad, CA). Next, a segment of the *ABCA12* cDNA was PCR-amplified with primers 5′-TCCGTCATCCTCACATCTTCA-3′ (forward) and 5′-GAACCTTGGCTGCTGGTATC-3′ (reverse) using Go-Taq polymerase (Promega, Charbonnières, France). The cDNA amplimers were cloned into PGEM-T vector (Promega, Charbonnières, France) and sequenced using the SP6 primer (5′-ATTTAGGT GACACTATAGAATAC-3′) and the T7 primer (5′-GTAATACGACT CACTATAGGGC-3′). In parallel, the cDNA amplimers were analyzed on standard agarose gel and by capillary electrophoresis on an ABI 310 Genetic Analyzer running the GeneScan software (Applied Biosystems, Foster City, CA).

Immunohistological and immunoblot analysis of ABCA12 protein expression

Immunodetection of ABCA12 was performed using an affinity purified anti-ABCA12 serum raised in rabbits using a 14 amino-acid sequence synthetic peptide (residues 2,567–2,580) derived from the ABCA12 sequence (NM 173076) as the immunogen (Akiyama *et al.*, 2005). Immunofluorescent labeling was performed as described previously (Akiyama *et al.*, 2000). Briefly, 6-μm-thick sections of fresh patient's skin were cut using a cryostat. The sections were incubated in primary antibody solution, anti-ABCA12 antiserum diluted 1/10, for 1 hour at 37°C. The sections were then incubated in FITC-conjugated goat anti-rabbit Igs diluted 1:100 (DAKO, Glostrup, Denmark) for 30 minutes at room temperature, followed by nuclear counterstain by propidium iodide (Sigma Chemical Co., St Louis, MO). The sections were extensively washed with phosphate-buffered saline between incubations. The stained sections were then mounted with a coverslip and observed using a confocal laser scanning microscope. For Western blot analysis, proteins were extracted from cultured keratinocytes in the presence of protease inhibitors (Complete Mini Protease Inhibitor Cocktail, Roche Diagnostics, Meylan, France), fractionated by SDS-PAGE using 30 μg/lane protein on a 4% gel, and transferred to a nitrocellulose membrane (Hybond-C Extra, Amersham Biosciences, Saclay, France). Membrane blocking and incubation with antibody (1:5,000) were carried out in phosphate-buffered saline with 5% skim milk. Secondary antibody was goat anti-rabbit IgG antibodies conjugated to horseradish peroxidase (1:5000, Cell Signalling Technology, Beverley). Signals were revealed with ECL + chemiluminescence reagents (GE Healthcare Bio-Sciences Corp., Piscataway, NJ).

Informed consent was obtained from the patients' parents. This study was approved by the medical ethical committees at the Hokkaido University, Sapporo, Japan, Purpan Hospital, Toulouse, France and Nantes University Hospital, Nantes, France. The study was conducted according to the Declaration of Helsinki Principles.

CONFLICT OF INTEREST

The authors state no conflict of interest.

ACKNOWLEDGMENTS

We thank Ms Megumi Sato, Ms Akari Nagasaki, and Ms Anne-Marie Mazarguil for their technical assistance on this project. This work was supported in part by The GENESKIN European project, the French Ministry of Health (Reference center for orphan skin diseases), Grants-in-Aid from the Ministry of Education, Science, Sports, and Culture of Japan to M. Akiyama (Kiban B. 16390312 and Kiban B. 18390310).

REFERENCES

Akiyama M (2006) Pathomechanisms of harlequin ichthyosis and ABCA transporters in human diseases. *Arch Dermatol* 142:914–8

Akiyama M, Dale BA, Smith LT, Shimizu H, Holbrook KA (1998) Regional difference in expression of characteristic abnormality of harlequin ichthyosis in affected fetuses. *Prenat Diagn* 18:425–36

Akiyama M, Kim D-K, Main DM, Otto CE, Holbrook KA (1994) Characteristic morphologic abnormality of harlequin ichthyosis detected in amniotic fluid cells. *J Invest Dermatol* 102:210–3

Akiyama M, Sakai K, Sugiyama-Nakagiri Y, Yamanaka Y, McMillan JR, Sawamura D *et al.* (2006a) Compound heterozygous mutations including a *de novo* missense mutation in *ABCA12* led to a case of harlequin ichthyosis with moderate clinical severity. *J Invest Dermatol* 126:1518–23

Akiyama M, Sakai K, Wolff G, Hausser I, McMillan JR, Sawamura D *et al.* (2006b) A novel ABCA12 mutation 3270delT causes harlequin ichthyosis. *Br J Dermatol* 155:1064–6

Akiyama M, Smith LT, Shimizu H (2000) Changing patterns of localization of putative stem cells in developing human hair follicles. *J Invest Dermatol* 114:321–7

Akiyama M, Sugiyama-Nakagiri Y, Sakai K, McMillan JR, Goto M, Arita K *et al.* (2005) Mutations in ABCA12 in harlequin ichthyosis and functional rescue by corrective gene transfer. *J Clin Invest* 115:1777–84

Akiyama M, Suzumori K, Shimizu H (1999) Prenatal diagnosis of harlequin ichthyosis by the examinations of keratinized hair canals and amniotic fluid cells at 19 weeks' estimated gestational age. *Prenat Diagn* 19:167–71

Annilo T, Shulenin S, Chen ZQ, Arnould I, Prades C, Lemoine C *et al.* (2002) Identification and characterization of a novel ABCA subfamily member, ABCA12, located in the lamellar ichthyosis region on 2q34. *Cytogenet Genome Res* 98:166–9

Barrandon Y, Green H (1987) Cell migration is essential for sustained growth of keratinocyte colonies: the roles of transforming growth factor-alpha and epidermal growth factor. *Cell* 50:1131–7

Blanchet-Bardon C, Dumez YFL, Lutzner MA, Puissant A, Henrion R, Bernheim A (1983) Prenatal diagnosis of harlequin fetus. *Lancet* 1:132

Dale BA, Holbrook KA, Fleckman P, Kimball JR, Brumbaugh S, Sybert VP (1990) Heterogeneity in harlequin ichthyosis, an inborn error of epidermal keratinization: variable morphology and structural protein expression and a defect in lamellar granules. *J Invest Dermatol* 94:6–18

Holbrook KA, Odland GF (1978) Structure of the human fetal hair canal and initial hair eruption. *J Invest Dermatol* 71:385–90

Holbrook KA, Odland GF (1980) Regional development of the human epidermis in the first trimester embryo and the second trimester fetus (ages related to the timing of amniocentesis and fetal biopsy). *J Invest Dermatol* 74:161–8

Kelsell DP, Norgett EE, Unsworth H, Teh M-T, Cullup T, Mein CA *et al.* (2005) Mutations in ABCA12 underlie the severe congenital skin disease harlequin ichthyosis. *Am J Hum Genet* 76:794–803

Lefèvre C, Audebert S, Jobard F, Bouadjar B, Lakhdar H, Boughdene-Stambouli O *et al.* (2003) Mutations in the transporter ABCA12 are associated with lamellar ichthyosis type 2. *Hum Mol Genet* 12: 2369–78

Nalla VK, Rogan PK (2005) Automated splicing mutation analysis by information theory. *Hum Mutat* 25:334–42

Shimizu A, Akiyama M, Ishiko A, Yoshiike T, Suzumori K, Shimizu H (2005) Prenatal exclusion of harlequin ichthyosis; potential pitfalls in the timing of the fetal skin biopsy. *Br J Dermatol* 153:811–4

Shimizu H, Suzumori K (1999) Prenatal diagnosis as a text for genodermatoses: its past, present and future. *J Dermatol Sci* 19:1–8

Suzumori K, Kanzaki T (1991) Prenatal diagnosis of harlequin ichthyosis by fetal skin biopsy; report of two cases. *Prenat Diagn* 11:451–7

Tsuji-Abe Y, Akiyama M, Nakamura H, Takizawa Y, Sawamura D, Matsunaga K *et al.* (2004) DNA-based prenatal exclusion of bullous congenital ichthyosiform erythroderma at the early stage, 10-11 weeks' of pregnancy in two consequent siblings. *J Am Acad Dermatol* 51:1008–11

Uitto J (2005) The gene family of ABC transporters – novel mutations, new phenotypes. *Trends Mol Med* 11:341–3

Uitto J, Pfendner E, Jackson LG (2003) Probing the fetal genome: progress in non-invasive prenatal diagnosis. *Trends Mol Med* 9:339–43

Williams ML, Elias PM (1987) Genetically transmitted, generalized disorders of cornification; the ichthyoses. *Dermatol Clin* 5:155–78

Case Report

Dermatology

Dermatology 2007;215:155–159
DOI: 10.1159/000104269

Received: December 21, 2006
Accepted: February 20, 2007

Compound Heterozygous *ABCA12* Mutations Including a Novel Nonsense Mutation Underlie Harlequin Ichthyosis

Masashi Akiyama[a] Kaori Sakai[a] Toshihiro Sato[b] James R. McMillan[a] Maki Goto[a]
Daisuke Sawamura[a] Hiroshi Shimizu[a]

[a]Department of Dermatology, Hokkaido University Graduate School of Medicine, Sapporo, and
[b]Division of Dermatology, Oita Prefectural Hospital, Oita, Japan

Key Words
ATP-binding cassette transporter · Barrier function · Lipid · Retinoid

Abstract
Recently, it has been reported that several harlequin ichthyosis (HI) patients survive the neonatal period and their condition subsequently improves. Here we describe a 2-year-old Japanese boy who exhibited typical clinical features of HI at birth. He survived beyond the neonatal period after oral retinoid treatment and, at the age of 2 years, showed moderately thick, lamellar scales and erythroderma over his whole body. The patient is a compound heterozygote for 2 *ABCA12* mutations, a paternal deletion mutation c.2021_2022del (p.Lys674ArgfsX63) and a novel maternal nonsense mutation c.7444C → T (p.Arg2482X). Electron microscopic observation of a skin biopsy specimen from the perinatal period revealed epidermal ultrastructural features consistent with HI. Immunofluorescence labeling using antiserum against a C-terminal ABCA12 epitope showed loss of expression in the patient's epidermis. The present patient demonstrates that rapid diagnosis of HI by ABCA12 expression analysis and mutation detection, and early commencement of systemic retinoid therapy are crucial to significantly improving an HI patient's prognosis.

Introduction

Harlequin ichthyosis (HI) is a severe and often fatal congenital ichthyosis with an autosomal recessive inheritance pattern [1]. Clinical features include thick, plate-like scales with ectropion, eclabium and flattened ears. It was reported that the pathomechanism underlying HI results from defective function of the lipid transporter ABCA12, which causes abnormal lamellar granule lipid transport in keratinocytes, and a malformation of the epidermal lipid barrier [2]. Another group independently reported *ABCA12* mutations in HI after linkage analysis [3]. Until the 1980s, newborns affected with HI rarely survived beyond the neonatal period. However, recently, HI babies often have a better prognosis [4–8]. In order to obtain clues to determine the definitive features of HI patients with a better prognosis, we report an HI male patient with compound heterozygous *ABCA12* mutations including a novel nonsense mutation leading to the typical HI phenotype presentation at birth. The patient survived and later showed lamellar scales on a background of erythematous skin over his entire body.

Case Report

The patient, a 2-year-old boy, was the first child of healthy, unrelated Japanese parents. There was no family history of any related disorders. Both parents of the patient had no hyperkeratotic skin lesion at all. At birth, his entire body surface was covered with large, thick, plate-like scales, partly bordered by irregular fissures (fig. 1). Severe ectropion and eclabium were seen. The fingers and toes were partly mutilated by the thick scales. The patient was transferred to neonatal intensive care unit and cared for with local application of emollient ointment in a humid incubator. From the 15th day of life, just after the skin biopsy had been performed, oral retinoid treatment was started at 1 mg/kg. The plate-like scales were carefully peeled off and the patient showed relatively thinner scales gradually forming on a background of erythrodermic skin of the whole body at 1 year and 9 months of age. Subsequently his general condition improved and the retinoid dose was reduced to 0.5 mg/kg. At the age of 2 years, the patient showed moderately thick, lamellar scales and erythroderma on his entire body (fig. 2).

A skin biopsy sample, taken from the right thigh at 14 days of age, showed compact and severe hyperkeratosis. Electron microscopy revealed numerous abnormal lamellar granules in the granular layer ke-

KARGER
Fax +41 61 306 12 34
E-Mail karger@karger.ch
www.karger.com

1018–8665/07/2152–0155$23.50/0

Accessible online at:
www.karger.com/drm

Masashi Akiyama, MD, PhD
Department of Dermatology
Hokkaido University Graduate School of Medicine
North 15 West 7, Kita-ku, Sapporo 060-8638 (Japan)
Tel. +81 11 716 1161, ext. 5962, Fax +81 11 706 7820, E-Mail akiyama@med.hokudai.ac.jp

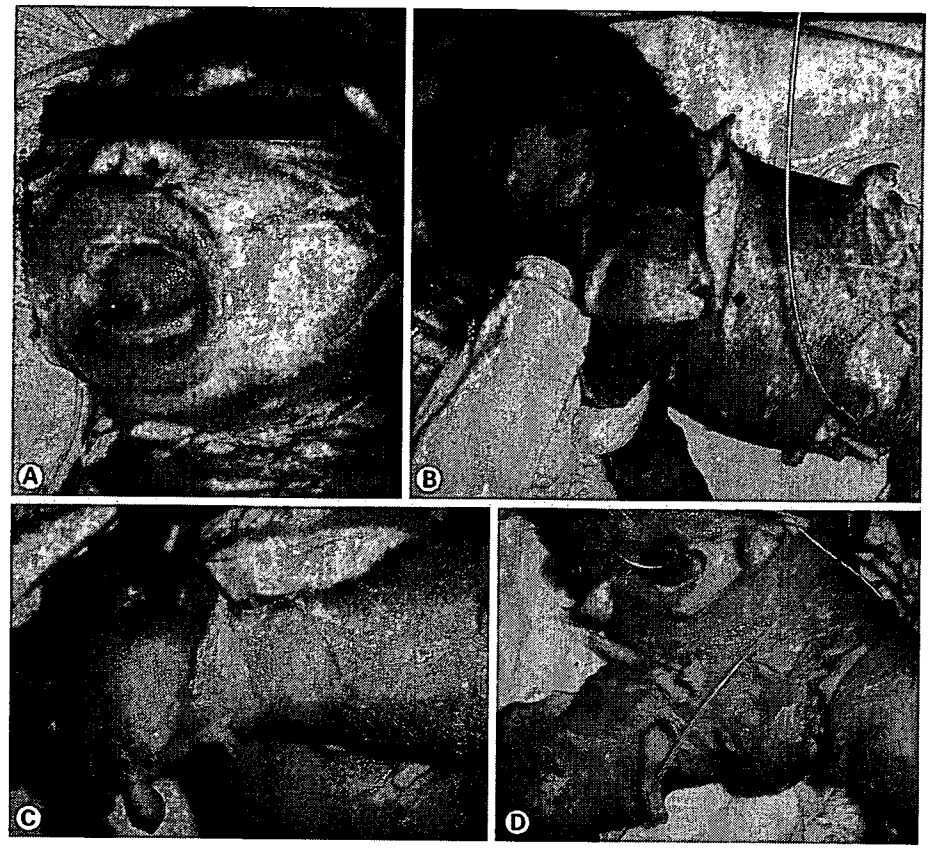

Fig. 1. The patient showed the typical HI phenotype in the neonatal period. **A** Severe eclabium and ectropion of the face. **B** Plate-like scales on a background of erythrodermic skin on the trunk and the arm. **C** Thick scales on the forearm and partly scale-mutilated fingers. **D** Plate-like scales peeling off from the erythematous underlying skin on the lower abdomen and the thigh.

ratinocytes and a large number of lipid droplets with a variety of sizes in the epidermal cornified cells (fig. 3). These ultrastructural features were consistent with HI.

To elucidate the precise genetic abnormality in the family, mutation analysis was performed in the affected boy and both his parents. Briefly, genomic DNA isolated from peripheral blood cells was subjected to PCR amplification, followed by direct automated sequencing using an ABI PRISM 3100 genetic analyzer (ABI Advanced Biotechnologies, Columbia, Md., USA). Oligonucleotide primers and PCR conditions used for amplification of all exons and exon/intron borders of *ABCA12* were originally derived from the report by Lefèvre et al. [9] and were partially modified for the present study [2]. The entire coding region including the intron/exon boundaries for both forward and reverse DNA strands from the patient, his parents and 50 healthy Japanese controls were sequenced. In the patient, a combination of 2 heterozygous mutations, c.2021_2022del (p.Lys674Argfs X63) in exon 16 and a novel nonsense mutation c.7444C → T (p.Arg2482X) in exon 51, were identified (sequence according to GenBank accession No. NM173076) (fig. 4). The mutation c.2021_2022del was present in his father and the mutation c.7444C → T was demonstrated in his mother. The presence of both mutations was excluded in 100 alleles of 50 normal unrelated Japanese individuals.

Immunofluorescence studies using antiserum against epitopes in the C-terminal region of ABCA12 [2] revealed that ABCA12 staining was absent in the patient's epidermis, although ABCA12 staining was seen in the normal control epidermis, mainly in the granular layer (fig. 5).

Discussion

The ATP-binding cassette transporter superfamily is one of the largest gene families, encoding a highly conserved group of proteins involved in energy-dependent (active) transport of a variety of substrates across membranes [10, 11]. The ABCA subfamily, of which the *ABCA12* gene is a member, is assumed to be involved in lipid transport [12]. Mutations in these genes underlie several human genetic diseases [13–15]. In HI, serious *ABCA12* mutations cause abnormal lipid transport via lamellar granules in keratinocytes, resulting in the malformation or improper assembly of the epidermal keratinocyte surface lipid barrier [2].

The paternal deletion mutation c.2021_2022del (p.Lys674ArgfsX63) in exon 16 was reported in an unrelated Japanese family with HI [2]. This deletion mutation leads to a frame shift and introduces a stop codon at codon position 736, within the N-terminal intracytoplasmic domain of the ABCA12 protein. According to the molecular structure [16], this deletion mutation results in a serious truncation of ABCA12 peptide losing both ATP-binding cassettes, and is thought to critically affect the function of the ABCA12 protein.

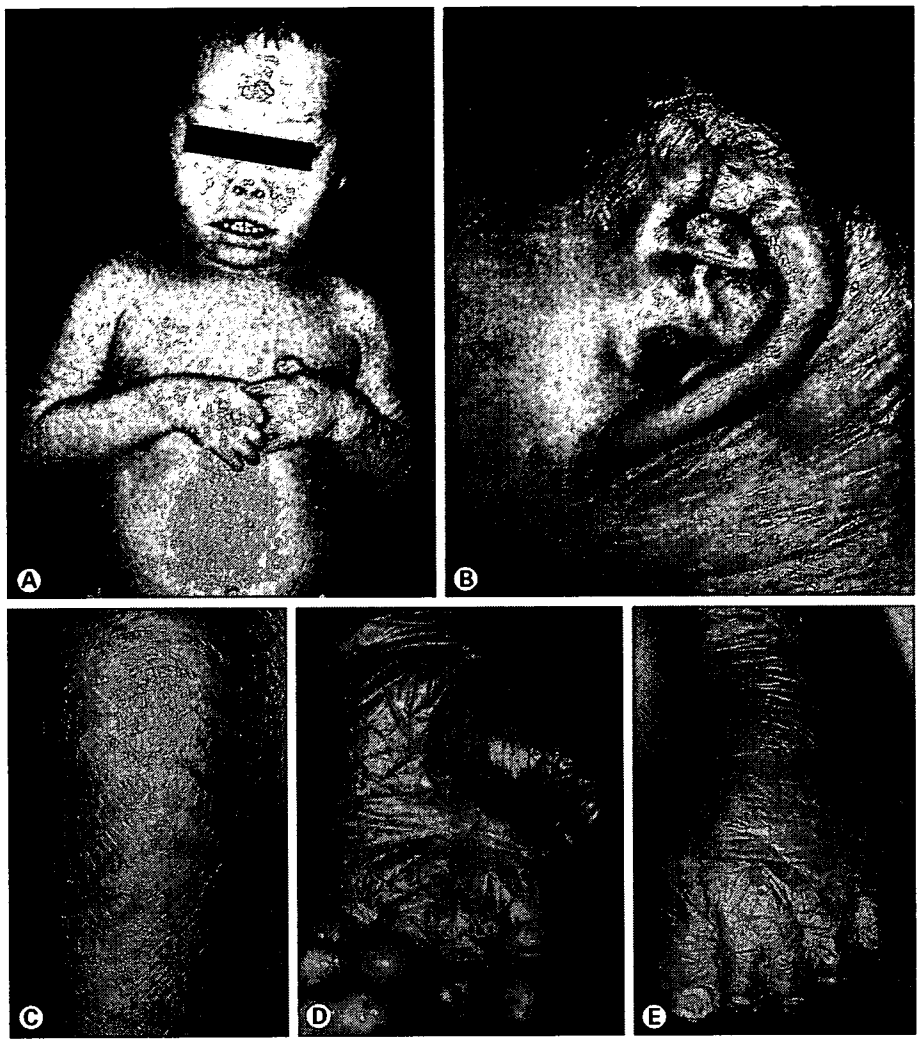

Fig. 2. The clinical features had improved by 2 years of age. **A** White to gray-white scales on the erythrodermic skin of the face and the upper half of the body. **B** Malformed pinna. **C–E** Thin white-gray scales on the upper arm (**C**), the palm (**D**) and the dorsa of the foot (**E**).

The maternal mutation c.7444C → T (p.Arg2482X) in exon 51 leads to a change of the arginine residue at codon 2482 into a stop codon and this premature translation termination eliminates 114 amino acids at the C-terminus of ABCA12 polypeptide. Furthermore, the message from this mutant may be strikingly reduced by nonsense-mediated mRNA decay. Thus, this mutation is expected to abolish ABCA12 function.

The absence of expression of full length ABCA12 peptide in the patient's epidermis was confirmed by immunofluorescence analysis. No antigenic peptide was detected by the anti-ABCA12 antiserum in agreement with the theoretical deletion of the epitopes recognized by the antiserum in the compound heterozygous ABCA12 mutants. We do not have any data whether truncated ABCA12 polypeptides were expressed or not.

Concerning the genotype/phenotype correlation in *ABCA12* mutations, generally, homozygotes or compound heterozygotes of truncation mutations of *ABCA12*, such as the present case, lead to HI phenotype, and homozygotes or compound heterozygotes of missense mutations causing single amino acid alterations result in a lamellar ichthyosis or nonbullous congenital ichthyosiform erythroderma phenotype, although a few exceptional cases have been reported. Our patient survived beyond the perinatal and neonatal periods, probably in part due to the oral retinoid treatment. The patient is now 2 years old and his general condition is relatively good, although he has the clinical features of moderately thick, lamellar scales on a background of generally erythematous skin over his entire body.

Recently, the prognosis of newborns affected with HI has improved, owing to remarkable progress in neonatal intensive care and earlier, targeted oral retinoid treatment [4–8]. More than half of HI newborns including cases with a serious functional loss of ABCA12 can now survive beyond the perinatal period [7, 8, 15]. The exact reasons for the improved prognosis of our HI patient are unknown, whether it was due to the nature of the mutations or to the successful intensive care and retinoid treatment during the perinatal period or some combination of the two. After surviving the neonatal period, sev-

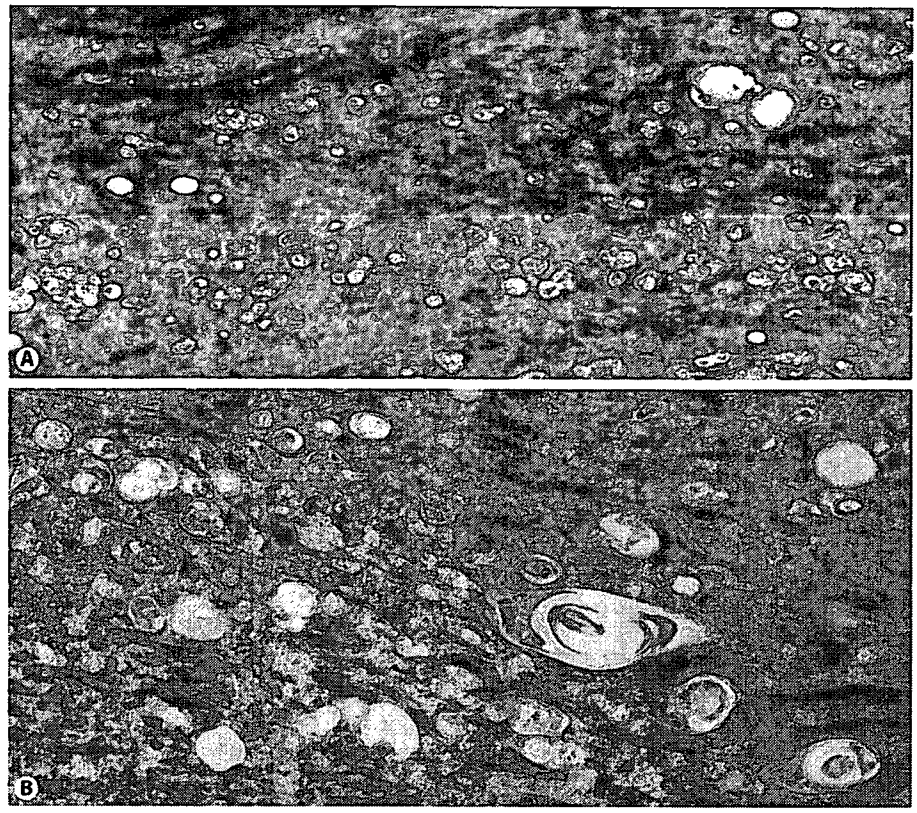

Fig. 3. Electron microscopic features of the patient's skin. **A** Abnormal lipid droplets accumulated in the cornified cells of the patient's epidermis. **B** Abnormal lamellar granules in the granular layer cells of the patient. **A** ×12,000. **B** ×30,000.

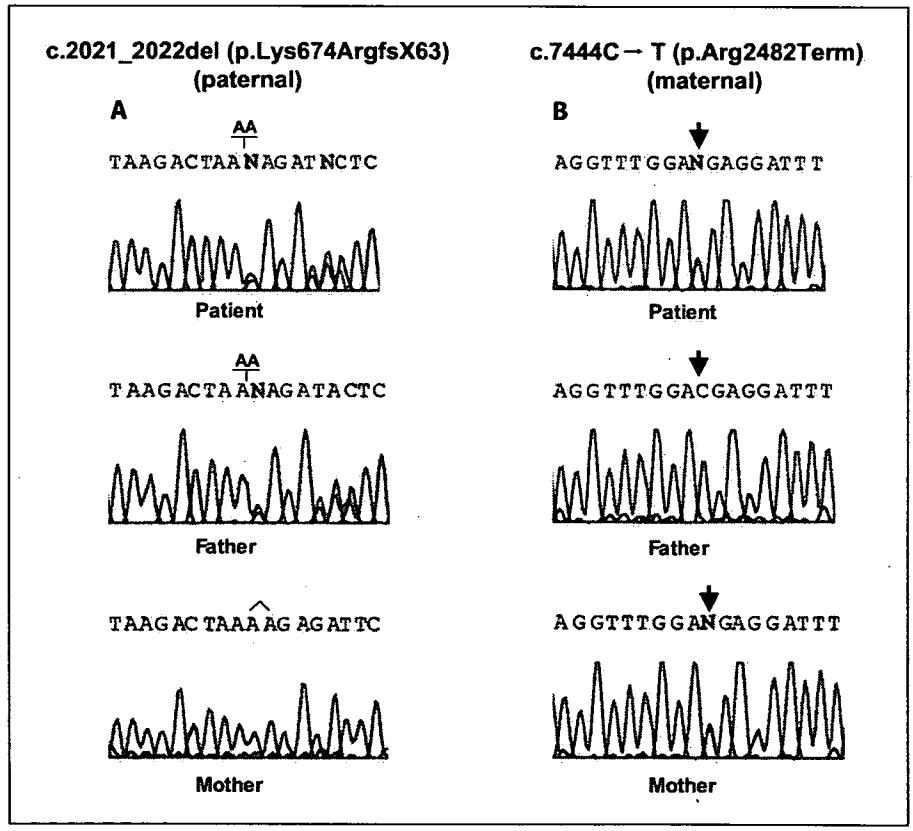

Fig. 4. Compound heterozygous *ABCA12* mutations in the patient. A combination of 2 heterozygous mutations, c.2021_2022del (p.Lys674ArgfsX63) in exon 16 (**A**) and a novel nonsense mutation c.7444C → T (p.Arg2482X) in exon 51 (**B**), were identified. The mutation c.2021_2022del was identified in his father, and the mutation c.7444C → T was demonstrated in his mother.

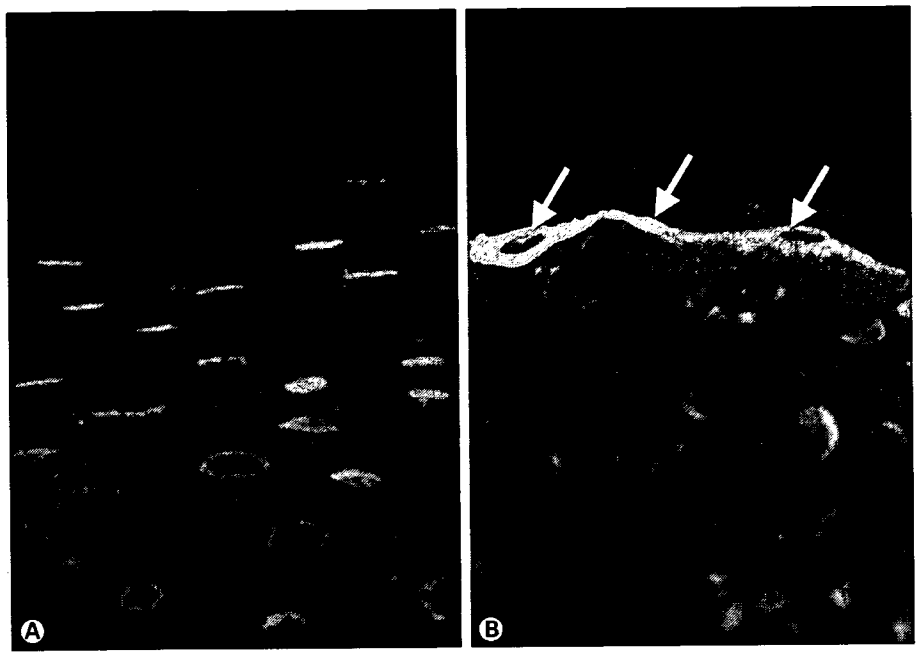

Fig. 5. Absence of ABCA12 immunostaining in the patient's epidermis. **A** In the patient's upper epidermis, very little or no ABCA12 immunostaining was seen in the keratinocyte cytoplasm. **B** In normal control human epidermis, ABCA12 labeling was seen in the granular layer keratinocytes (arrows). ABCA12, FITC (green); nuclear staining, propidium iodide (red). ×250.

eral HI patients' general condition improves [7, 8, 15]. The present case and a review of the literature indicate that the rapid diagnosis of HI by ABCA12 expression and mutation analyses and the early start of systemic retinoids are crucial and may drastically improve the prognosis and quality of life of patients with HI, although we do not have sufficient evidence to evaluate the effectiveness and necessity of early retinoid treatment in HI babies. Thus, we think that, in each HI case, we should determine carefully whether we introduce early retinoid treatment or not. Accumulation of greater numbers of similar cases is needed to further discuss genotype/phenotype correlations and the quality of life prognosis for HI patients.

Acknowledgments

We thank Ms. Satoko Ishikawa, Ms. Akari Nagasaki and Ms. Megumi Sato for their fine technical assistance on this project.

This work was supported in part by Grant-in-Aid from the Ministry of Education, Science, Sports and Culture of Japan to M.A. (Kiban B 18390310).

References

1 Akiyama M: Harlequin ichthyosis and other autosomal recessive congenital ichthyoses: the underlying genetic defects and pathomechanisms. J Dermatol Sci 2006;42:83–89.
2 Akiyama M, Sugiyama-Nakagiri Y, Sakai K, et al: Mutations in ABCA12 in harlequin ichthyosis and functional rescue by corrective gene transfer. J Clin Invest 2005;115:1777–1784.
3 Kelsell DP, Norgett EE, Unsworth H, et al: Mutations in ABCA12 underlie the severe congenital skin disease harlequin ichthyosis. Am J Hum Genet 2005;76:794–803.
4 Roberts LJ: Long-term survival of a harlequin fetus. J Am Acad Dermatol 1989;21:335–339.
5 Haftek M, Cambazard F, Dhouailly D, Réano A, Simon M, Lachaux A, Serre G, Claudy A, Schmitt D: A longitudinal study of a harlequin infant presenting clinically as non-bullous congenital ichthyosiform erythroderma. Br J Dermatol 1996;135:448–453.
6 Singh S, Bhura M, Maheshwari A, et al: Successful treatment of harlequin ichthyosis with acitretin. Int J Dermatol 2001;40:472–473.
7 Akiyama M, Sakai K, Sugiyama-Nakagiri Y, Yamanaka Y, McMillan JR, Sawamura D, Niizeki H, Miyagawa S, Shimizu H: Compound heterozygous mutations including a de novo missense mutation in *ABCA12* led to a case of harlequin ichthyosis with moderate clinical severity. J Invest Dermatol 2006;126:1518–1523.
8 Akiyama M, Sakai K, Wolff G, Hausser I, McMillan JR, Sawamura D, Shimizu H: A novel ABCA12 mutation 3270delT causes harlequin ichthyosis. Br J Dermatol 2006;155:1064–1066.
9 Lefèvre C, Audebert S, Jobard F, et al: Mutations in the transporter ABCA12 are associated with lamellar ichthyosis type 2. Hum Mol Genet 2003;12:2369–2378.
10 Borst P, Elferink RO: Mammalian ABC transporters in health and disease. Annu Rev Biochem 2002;71:537–592.
11 Uitto J: The gene family of ABC transporters – novel mutations, new phenotypes. Trends Mol Med 2005;11:341–343.
12 Peelman F, Labeur C, Vanloo B, et al: Characterization of the ABCA transporter subfamily: identification of prokaryotic and eukaryotic members, phylogeny and topology. J Mol Biol 2003;325:259–274.
13 Klein I, Sarkadi B, Varadi A: An inventory of the human ABC proteins. Biochim Biophys Acta 1999;1461:237–262.
14 Shulenin S, Nogee LM, Annilo T, Wert SE, Whitsett JA, Dean M: ABCA3 gene mutations in newborns with fatal surfactant deficiency. N Engl J Med 2004;350:1296–1303.
15 Akiyama M: Pathomechanisms of harlequin ichthyosis and ABCA transporters in human diseases. Arch Dermatol 2006;142:914–918.
16 Annilo T, Shulenin S, Chen ZQ, et al: Identification and characterization of a novel ABCA subfamily member, ABCA12, located in the lamellar ichthyosis region on 2q34. Cytogenet Genome Res 2002;98:169–176.

SHORT REPORT

ABSTRACT: Recently, mutations in *PNPLA2* encoding adipose triglyceride lipase (ATGL) were reported to underlie a neutral lipid storage disease (NLSD) subgroup characterized by mild myopathy and the absence of ichthyosis. In the present study a novel homozygous *PNPLA2* mutation c.475_478dupCTCC (p.Gln160ProfsX19) in the patatin domain, the ATGL active site, was detected in a woman with NLSD and severe myopathy. The present results suggest that a premature truncation mutation in the patatin domain causes NLSD with severe myopathy.

Muscle Nerve **36**: 856–859, 2007

NOVEL DUPLICATION MUTATION IN THE PATATIN DOMAIN OF ADIPOSE TRIGLYCERIDE LIPASE (PNPLA2) IN NEUTRAL LIPID STORAGE DISEASE WITH SEVERE MYOPATHY

MASASHI AKIYAMA, MD, PhD,[1] KAORI SAKAI, MS,[1] MASAYA OGAWA, MD, PhD,[2] JAMES R. McMILLAN, PhD,[1] DAISUKE SAWAMURA, MD, PhD,[3] and HIROSHI SHIMIZU, MD, PhD[1]

[1] Department of Dermatology, Hokkaido University Graduate School of Medicine, N15 W7, Sapporo 060-8638, Japan
[2] Department of Neurology, Aomori Prefectural Central Hospital, Aomori, Japan
[3] Department of Dermatology, Hirosaki University Graduate School of Medicine, Hirosaki, Japan

Accepted 20 June 2007

A subgroup of neutral lipid storage diseases (NLSDs), Dorfman–Chanarin syndrome (MIM 275630), is defined as an NLSD with ichthyosis, often also associated with liver dysfunction, cirrhosis, and mild mental retardation and, occasionally, with mild myopathy.[2,3] Dorfman–Chanarin syndrome is caused by mutations in *CGI-58/ABHD5*.[1,11] The adipose triglyceride lipase (ATGL) enzyme encoded by the gene *PNPLA2* is activated by *CGI-58*[10] and, recently, mutations in ATGL were reported to underlie NLSD with mild myopathy and an absence of ichthyosis.[4]

In the initial NLSD *PNPLA2* mutation report,[4] no *PNPLA2* mutations were identified affecting the patatin domain and all three patients showed only mild myopathy. In the current investigation we report a case of NLSD with severe myopathy that was attributed to a *PNPLA2* premature truncation mutation affecting the patatin domain.

Abbreviations: ATGL, adipose triglyceride lipase; NLSD, neutral lipid storage disease
Key words: ATGL; myopathy; patatin; PNPLA2
Correspondence to: M. Akiyama; e-mail: akiyama@med.hokudai.ac.jp

Published online 26 July 2007 in Wiley InterScience (www.interscience.wiley.com). DOI 10.1002/mus.20869

CASE REPORT

A 35-year-old Japanese woman was the sixth child born at term to healthy, nonconsanguineous parents, both from a small village in the northern part of Japan. Pregnancy and delivery were uneventful. She has three sisters and three brothers, all apparently healthy, and a younger brother who died from an unknown medical condition at the age of 5. She showed delays in walking, and from childhood was slow in running.

At the age of 30 she presented with recurrent dislocation of her right shoulder joint. At 33 she noticed weakness of all extremities and could not raise her arms. The limb weakness gradually worsened, resulting in a gait disturbance at the age of 35. She had no gastrointestinal symptom. On neurological examination at the age of 35 her mental status and cranial nerve function were normal. She showed diffuse muscle wasting and severe muscle weakness. She could not raise her arms at all and showed Gowers' sign and a waddling gait, indicating proximally dominant muscle weakness. Deep tendon reflexes were absent and plantar responses were flexor. Sensory disturbance was not seen. Ichthyosis, hearing loss, ocular anomalies, ataxia, short-stature, or microcephaly were not observed.

Laboratory tests showed increased serum concentrations of creatine kinase (654 IU/L; normal, 44–

170 IU/L). Serum lactic acid, pyruvic acid, and carnitine levels were within the normal range. She did not have hyperglycemia or hyperlipemia. An aerobic exercise test was normal and a fasting test showed increased serum concentrations of ketone bodies, suggesting no mitochondrial dysfunction. Needle electromyography revealed myogenic changes; motor unit potentials were diminished in amplitude and duration, resulting in spiky units during voluntary contraction. Echocardiography was normal and Holter ECG showed occasional ventricular premature contractions. Echograms of the abdomen showed neither hepatomegaly nor fatty liver, although splenomegaly was seen. Skeletal-muscle computed tomography showed an extensive degeneration with fatty replacement in deltoid, biceps brachii, hamstring, and gastrocnemius, although triceps brachii and quadriceps femoris were less impaired.

A muscle biopsy of the rectus femoris revealed abundant neutral lipid droplets in the sarcoplasm (Fig. 1A,B), which were consistent with a lipid-storage myopathy. In peripheral blood smears, neutral lipid vacuoles were observed in leukocytes (Jordans' anomaly) (Fig. 1C). The patient was diagnosed as having NLSD without ichthyosis.

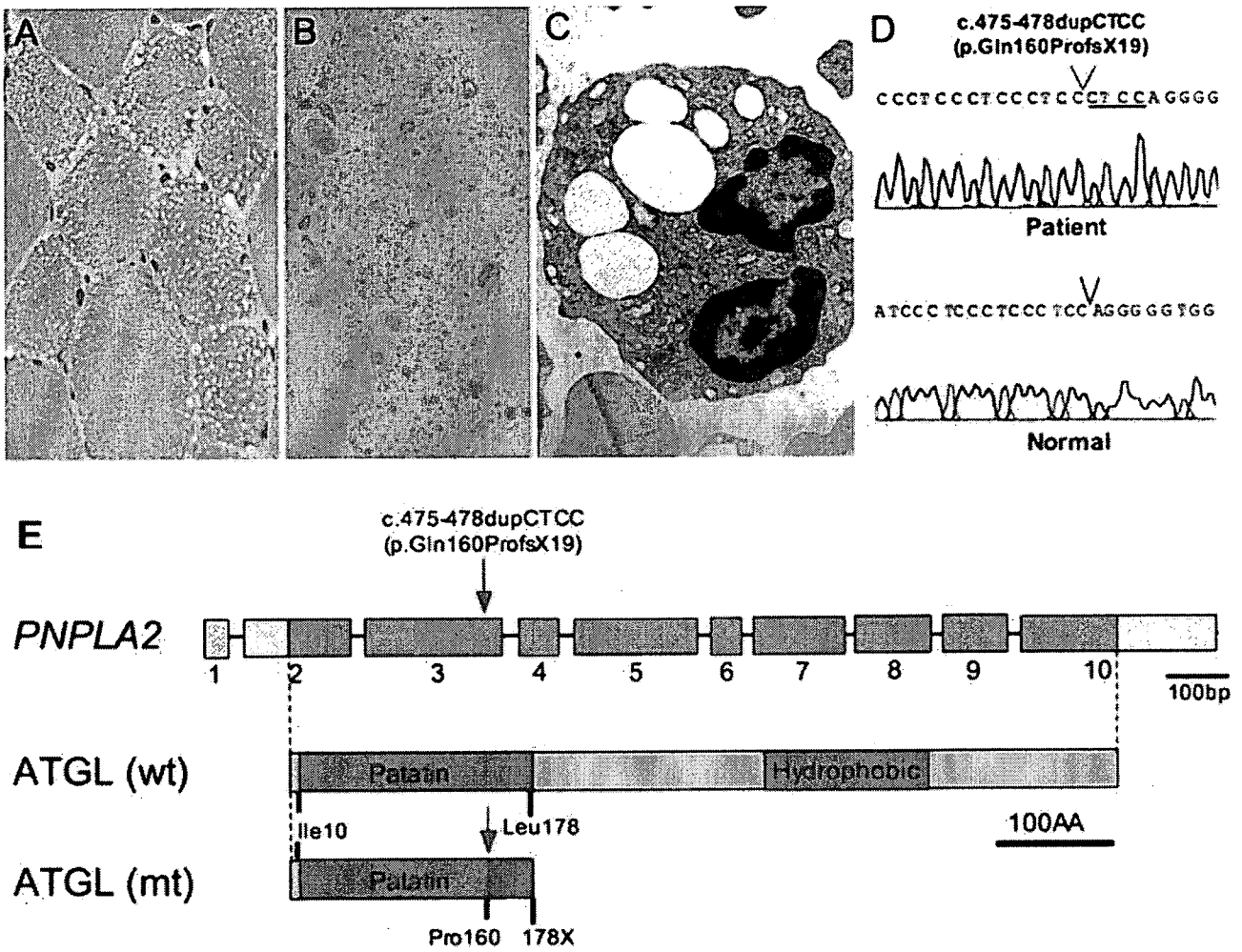

FIGURE 1. Neutral lipid accumulation and a *PNPLA2* mutation in a patient with NLSD and myopathy. **(A)** Hematoxylin and eosin–stained sections of muscle revealed vacant vacuoles in the muscle cells. **(B)** Light microscopy of frozen transverse sections of skeletal muscle stained by oil red O. Cytoplasmic droplets contained neutral lipids (triglycerides) (orange). **(C)** Electron microscopic observations revealed vacant vacuoles in the cytoplasm of a peripheral blood leukocyte. **(D)** Electropherogram of the mutant alleles of *PNPLA2* from genomic DNA of the patient showed that the patient was homozygous for the 475_478CTCC duplication (c.475_478dupCTCC) in exon 4. **(E)** Predicted structure of ATGL and mutations in the *PNPLA2* gene in the present patient with NLSD and myopathy. Predicted structure of the wildtype (wt) ATGL, including the patatin (red) (PFAM accession PF01734) and hydrophobic (green) domains.[5] The sites of the mutation (red arrows), frameshifts (blue), and premature stop codon (178X) are indicated in the predicted structure of the truncated mutant (mt) ATGL encoded by mutated *PNPLA2* in the patient.